HHS Public Access

Author manuscript

J Control Release. Author manuscript; available in PMC 2021 April 10.

Published in final edited form as:

J Control Release. 2020 April 10; 320: 45–62. doi:10.1016/j.jconrel.2020.01.009.

Magnetic iron oxide nanoparticles for imaging, targeting and treatment of primary and metastatic tumors of the brain

Liron L. Israel, **Anna Galstyan**, **Eggehard Holler**, **Julia Y. Ljubimova***

Nanomedicine Research Center, Department of Neurosurgery, Cedars-Sinai Medical Center, 8700 Beverly Blvd, Los Angeles, CA 90048, USA

Abstract

Magnetic nanoparticles in general, and iron oxide nanoparticles in particular, have been studied extensively during the past 20 years for numerous biomedical applications. The main applications of these nanoparticles are in magnetic resonance imaging (MRI), magnetic targeting, gene and drug delivery, magnetic hyperthermia for tumor treatment, and manipulation of the immune system by macrophage polarization for cancer treatment. Recently, considerable attention has been paid to magnetic particle imaging (MPI) because of its better sensitivity compared to MRI. In recent years, MRI and MPI have been combined as a dual or multimodal imaging method to enhance the signal in the brain for the early detection and treatment of brain pathologies. Because magnetic and iron oxide nanoparticles are so diverse and can be used in multiple applications such as imaging or therapy, they have attractive features for brain delivery. However, the greatest limitations for the use of MRI/MPI for imaging and treatment are in brain delivery, with one of these limitations being the brain-blood barrier (BBB). This review addresses the current status, chemical compositions, advantages and disadvantages, toxicity and most importantly the future directions for the delivery of iron oxide based substances across the blood-brain barrier for targeting, imaging and therapy of primary and metastatic tumors of the brain

Keywords

Iron oxide; Brain tumor; Imaging; Therapy; Magnetic targeting

1. Introduction

Many pathological conditions of the central nervous system (CNS), including brain tumors, present a special challenge for imaging, therapy and drug delivery, since the brain is protected by the blood-brain barrier (BBB) which prevents many drugs from reaching a therapeutic level in the brain. The BBB is represented by endothelial cells (ECs) of the capillary wall with tight junctions between them, astrocyte end-feet surrounding the capillary, and pericytes embedded in the capillary basement membrane [1]. The main functions of the BBB are maintaining brain homeostasis and keeping potentially damaging

*Corresponding author.: Julia.Ljubimova@cshs.org (J.Y. Ljubimova).

Conflict of Interest

The authors declare no conflict of interest.

molecules out of the CNS. The BBB allows the passage of some molecules by passive diffusion as well as the selective transport of molecules such as glucose, water and amino acids that are crucial to neural function, but protects the CNS from exposure to harmful compounds and also prevents many therapeutic formulations from reaching their targets in the brain.

Some tumors, such as gliomas and metastatic tumors in the brain, are not accessible to chemotherapy, due to the BBB. There are different ways to bypass the BBB for chemotherapeutic medicines, such as the usage of iatrogenic agents or intrathecal drug administration; modalities for drug delivery to the brain in unit doses through the BBB entail its disruption by osmotic means or biochemically by the use of vasoactive substances such as bradykinin [2], or even by localized exposure to high-intensity focused ultrasound (HIFU) [3].

Other methods used to penetrate the BBB may involve the use of endogenous transport systems (including carrier-mediated transporters such as glucose and amino acid carriers), receptor-mediated transcytosis for insulin or transferrin, and the blocking of active efflux transporters (such as p-glycoprotein). However, vectors targeting BBB transporters, such as the transferrin receptor (TfR), have been found to remain entrapped in brain ECs or capillaries, instead of being ferried across the BBB into the targeted area [4,5]. Methods for drug delivery behind the BBB include intracerebral implantation (such as with needles) and convection-enhanced distribution. Mannitol can also be used to bypass the BBB.

However, all the above described mechanisms for delivery across the BBB are not sufficient for targeting and treatment of malignant gliomas. Malignant gliomas remain as aggressive and lethal primary brain tumors in adults. Glioblastoma (GBM) is the most common and highest grade malignant glioma. It is characterized by necrosis, intensive vascular proliferation (angiogenesis) and migration of cancer cells (invasion) [6]. Despite all the current treatment modalities, such as surgery, chemotherapy, and radiotherapy, there is no definitive treatment against malignant gliomas. They lead to an extremely high relapse rate and a median survival of 12–15 months after diagnosis [7–11].

Each of the therapeutic approaches mentioned above has particular restrictions. Brain tumors are often inaccessible and sometimes are not available for neurosurgeons during an operation [12,13]. In addition, GBM infiltrates the surrounding brain tissue, making complete resection impossible [14,15].

The most important limitations that prevent the successful use of chemotherapy are the intolerable side effects (high toxicity of drugs due to systemic distribution) imposed on patients [16] and delivery of drugs. The recommended high doses of radiotherapy are harmful for the healthy brain tissue around the tumor [17,18]. At this stage of treatment, the risk of relapse is unfortunately inevitable. These restrictions inherent in conventional brain tumor treatments encourage investigations of new methods for cancer therapy [19].

Nanotechnology-based delivery systems are being extensively studied for the effective treatment of brain tumors and reduction of side effects, enabling the combination of targeting, drug loading and drug releasing in large capacity. For these reasons, nanosystems

tend to be larger in size, making BBB penetration even more difficult to achieve. Therefore, a nanomaterial which can potentially be used for both treatment and imaging (also known as “theranostic” – therapy and diagnostic) and thus decrease the nanosystem size is of great interest.

In that regard the chemistry of iron is intriguing, partially because iron is an abundant element used in various fields. Moreover, there is growing interest in ferro- and ferrimagnetic materials for both technological and theoretical reasons, especially in the context of magnetic imaging and targeting [20–23].

Magnetically responsive magnetite (Fe_3O_4) and maghemite (γ-Fe_2O_3)-based crystalline particles can be readily prepared as nanoscale-sized formulations (3.0−100.0 nm). Because both of these iron oxides (IOs) contain atom vacancies and surface defects as well as polar amphoteric OH decoration, they are amenable to easy surface manipulation and functionalization [24–30].

Magnetite (Fe_3O_4) is easily obtained by co-precipitating aqueous Fe^{3+} and Fe^{2+} ions [31,32], microemulsions [33], laser pyrolysis [34] or thermal decomposition of iron acetyl acetonate ($Fe(acac)_3$) or similar species [35–37] (Fig. 1A). Magnetite has the particularity of containing both Fe^{2+} and Fe^{3+} cations within an inverse spinel structure. It is characterized by fast electron hopping between the iron cations on the octahedral sub-lattice, and is also very susceptible to oxidation. To utilize it for biomedical applications and reduce its toxicity, which usually originates from the presence of Fe^{2+} atoms, a stabilizing agent is often needed. Such an agent is usually a polymer such as a dextran coating/shell (used in the FDA approved formulation Feridex [ferumoxides]; a product since discontinued by the manufacturer) or small molecule stabilizers (e.g., ligands such as citric or oleic acid) [28,38–43].

Maghemite (γ-Fe_2O_3) is isostructural with magnetite but with cation vacancies, and with global properties which are quite similar, although maghemite is generally less magnetic but more stable than magnetite; it can be produced from the direct oxidation of magnetite [44,45] (Fig. 1A). Although maghemite does not always require a shell for stabilization, a shell or graft to the surface with polymers such as polyethylene glycol (PEG) [46] are often used in a biological system and increase the blood half-life of the nanoparticles (NPs). The increased half-life is usually due to postponing the opsonization process in which particles are targeted for destruction by phagocytic immune cells, which results in rapid clearance to the liver or spleen by the reticuloendothelial system (RES) [47,48]. Another way to increase the blood half-life is by adding a biomolecular corona that interacts with biological systems. This corona may thereby constitute a major element of the biological identity of the NP [49]. Inorganic coatings such as silica or gold are also used [21,50–52], as well as IO and graphene oxide combinations [53].

The biological activity and functionality, as well as the binding of any organic or inorganic ligand to the IO surface, depends on a variety of properties such as surface charge (zeta [ζ] potential), size, shape, surface functionalities and defects of the particle surface [24,54–61]. For example, metal doping of the surface allows ligands that use co-ordination chemistry

[24,62], while other surface functionalizations including polymeric coatings may allow covalent binding [25,63,64] (Fig. 1A). Electrostatic binding and complexation can also be used although they are generally considered less stable in the blood. For example, positively charged particles are often used to complex the negatively charged small interfering RNAs (siRNAs) for gene delivery [65]. Therefore, the IO-based nanomaterials which are intended for biomedical use are usually a nanocomposite system, often a core/shell system. Even though IO is usually used as the core or encapsulated within a polymeric NP, some systems with IO as the shell have also been studied (e.g. for potential use as magnetic resonance imaging [MRI] contrast agents) [63].

An example of an FDA approved formulation containing IO (often termed “ferro-fluids”) that is currently on the market is ferumoxytol (brand name: Feraheme) [66]. Its main application is in the treatment of anemia/iron deficiency, although it is also used as the core for nanocomposites in some drug development research studies. A study of ferumoxytol as a possible tumor treatment used the iron oxide nanoparticles (IONPs) to change macrophage polarization [67]. In a different study, ferumoxytol that was coated with a low molecular weight semi-synthetic carbohydrate (polyglucose sorbitol carboxymethyl ether) possessed potential imaging and hyperthermia properties. As for the crestline structure of the NP, in one study a method called selected area electron diffraction (SAED, an example can be seen in Fig. 1B) was used to show that the structure of ferumoxytol is consistent with the lattice spacing of cubic maghemite (γ-Fe_2O_3) cores [66]. However, in another study, where the IO material was initially considered to be either magnetite or maghemite, it was later determined to be magnetite, also according to SAED patterns [68]. The high similarity of the crystal structures of magnetite and maghemite, and hence the diffraction patterns make it difficult to distinguish between the two compounds.

Both magnetite and maghemite NPs are superparamagnetic (generally termed superparamagnetic iron oxide nanoparticles [SPIONs]), which means that at certain temperatures in the absence of an external magnetic field, their magnetization appears to be zero on average (i.e., in the superparamagnetic state). In this state, an external magnetic field can magnetize the NPs because their magnetic susceptibility is considered to be very high. This characteristic makes both magnetite and maghemite an excellent platform for magnetic targeting, magnetism-based hyperthermia and imaging, such as MRI or magnetic particle imaging (MPI). In addition to the two main basic structures of magnetite and maghemite, MFe_2O_4 structures are also often studied, where “M” is a metal other than iron (MFe_2O_4 is also the general form of magnetite, when M is Fe) [69].

For biomedical applications of IONPs, in addition to magnetic and crystalline properties, other characteristics such as the size, surface charge and lipophilicity must also be considered, as they can influence serum half-life and brain penetration [70–72]. In most cases, small-sized particles are preferred that could avoid activation of the complement system and RES clearance and have a greater ability to cross the BBB. As mentioned above, different types of surface coatings or surface functionalization can also address the issue of RES clearance. The surface charge is usually relevant to the specific biological application, since positively charged NPs will react with negatively charged biological structures such as siRNA and the cell membrane, thereby increasing the ability of the NPs to penetrate cells.

However, positively charged NPs may be cleared from the blood quickly and may also cause several complications such as hemolysis and platelet aggregation [70,73–75].

2. BBB in normal brain and in brain under pathological conditions

As mentioned above, the BBB is a general term for the functionalities which organize the permeability of blood vessels in the CNS to precisely regulate the transfer of molecules between the blood and the brain parenchyma [76,77]. The function of this barrier is to protect the brain from pathogens and neurotoxic molecules, as well as to maintain homeostasis. A blood vessel in the CNS is formed mainly by ECs connected by tight junctions (Fig. 2). These cells share a common basement membrane with pericytes. Neighboring astrocytes in combination with ECs, pericytes and neurons, and together with microglia (resident immune cells of the brain), are involved in brain immune responses [76,77]. Oxygen from the blood and carbon dioxide from the brain can diffuse freely, and small lipophilic molecules (typically with molecular weight less than 400 g/mol) can cross the BBB [78]. The BBB excludes most polar molecules, but certain nutrients and ions can gain access through the action of specific receptors [79].

While a normal BBB functions in healthy individuals, certain diseases can cause a dysfunction of the BBB. One of the fatal pathologies are brain tumors, either primary or metastatic. In cases of tumors in the CNS or other organs, normal angiogenesis is affected. The BBB is compromised, resulting in a “blood-tumor barrier”, often termed the BTB [80,81]. In this review, we use the term “BBB” and not “BTB” when discussing brain tumors, based on differences between brain and tumor microenvironments.

The BBB of intracranial tumors can be disrupted by fast angiogenesis. Leaky blood vessels of the growing tumor allow larger sized therapeutic agents including NPs or antibodies to access the interstitial portion of the tumor to some extent [79,82,83]. That phenomenon which is generally known in tumors as the “enhanced permeability and retention effect” (EPR), has also been studied as a delivery route for nanotherapeutics to brain tumors (“passive” targeting). However, most of these formulations did not pass clinical trials due to lack of efficacy, indicating that EPR alone was not sufficient to provide therapeutic levels in of these agents to brain tumors and besides, these agents caused toxicity and side effects [84].

In addition to “passive targeting” (i.e., EPR), “active” nano-based delivery systems have been developed using a brain vascular endothelial transcytosis mechanism [85]. The choice of the appropriate transcytosis system is important for efficient delivery through the BBB of a given tumor. Transcytosis receptors could be upregulated or downregulated in different brain tumors. For example, the TfR is upregulated in glioma and, therefore, nano drug delivery is chosen to select this receptor [86]. In contrast, the low density lipoprotein receptor related protein (LRP-1), another transcytosis receptor (discussed further below), is also overexpressed in glioma, but not in a brain metastatic tumor of lymphoma [87,88].

3. Techniques to deliver drugs across the BBB

3.1 Magnetic methods

One advantage of using IONPs is that magnetic methods can be used to make them cross the BBB. In one study, magnetic IONPs were “forced” to cross the BBB by applying a magnetic force generated by an external magnetic field that physically “pulled” the particles across the BBB [89]. A recent study [90] demonstrated that magnetic forces could be used for controlled drug delivery by disrupting endothelial cell-cell junctions. Although the work originally described was not aimed specifically for the BBB but for crossing endothelial barriers in general, the findings did provide some valuable mechanistic data relevant to crossing ECs of the BBB.

Such an *in vitro* magnetic switch of vascular permeability was investigated using an engineered endothelialized microfluidic system, which provided a tightly controlled flow environment mimicking the physiologic hemodynamic conditions in blood vessels [90]. For delivery, the authors designed nano vehicles consisting of synthesized magnetite nanocrystals (16 and 33 nm in diameter) which were fabricated via thermo-decomposition of $Fe(acac)_3$. The research strategy was that the force applied through intracellular magnetic NPs could trigger the reorganization of F-actin fibers and disrupt adherent endothelial junctions. F-actin is the major protein of muscle thin filaments and it is essential for important cellular functions such as the mobility and contraction of cells during cell division [91]. The data suggested that ECs are capable of simultaneously sensing both a mechanical, flow-induced shear stress and an intracellular magnetic NP induced force, whereby the combination and directions of these two forces modulate F-actin dynamics. In addition, when the intracellular magnetic force was large enough to induce a reversible change in the actin cytoskeleton, the changes in actin filaments led to a temporary disruption of adherent endothelial junctions rather than permanent alterations of the endothelial function. The authors concluded that by their technique the permeability of vascular endothelium could be increased using an external magnetic field to temporarily disrupt endothelial junctions through internalized IONPs and by this mechanism could activate a paracellular transport pathway to facilitate the local extravasation of circulating substances.

More specific studies of the IO method for crossing the BBB by using a magnetic field were published in the past decade [23,92,93]. In one recent example [94], SPIONs were prepared that had been synthesized by the decomposition of $Fe(acac)_3$ and coated with PEG, polyethylene imine (PEI), and Tween 80 (polysorbate 80), and were termed Tween-SPIONs. The authors demonstrated effective passage of tail-vein-injected Tween-SPIONs across the normal BBB in rats under an external magnetic field, with quantitative analyses showing significant accumulation of SPIONs in the cortex near the magnet, and progressively lower accumulation in brain tissues farther away from the magnet. Nevertheless, targeting across the BBB using IO combined with a magnetic field is still a challenging technique.

3.1.1. Methods using nonspecific mechanisms—Several methods can facilitate the crossing of the BBB without active targeting. One very common strategy is a simple adsorption mediated transcytosis. Vinzant et al. [95] relied on the observation that IONPs

can readily cross the intact BBB. Peptide cargo attached to maghemite NPs could be delivered into the brain without active targeting.

Another method [96,97] for crossing the BBB, also described in a study [98], applied a radio frequency (RF) field to cause the heating of commercial IONPs (hyperthermia) which had been administrated via the middle cerebral artery using a catheter. This technique enabled large dye molecules which were injected prior to IONPs to cross the BBB, which is then able to fully recover naturally after the treatment. Per the authors, magnetic NPs in this configuration act as miniaturized heat sources that deliver thermal energy uniquely to the endothelium with high spatial precision.

In another study [99], it was demonstrated that poly(butyl cyanoacrylate)-based microbubbles, carrying ultrasmall superparamagnetic iron oxide (USPIO) NPs, could be used to mediate and monitor BBB permeation. Upon exposure to transcranial ultrasound pulses, USPIO microbubbles are destroyed resulting in acoustic forces inducing vessel permeability. At the same time, USPIO NPs released from the microbubble shell cross the permeabilized BBB and accumulate in extravascular brain tissue. This method provided non-invasive r_2* based MRI information on the extent of BBB opening.

Sun et al. [100] used negatively charged IONPs in combination with lysophosphatidic acid (LPA, a phospholipid that signals extracellularly via cognate G protein-coupled receptors to mediate cellular processes) to transiently disrupt the tight junctions between ECs allowing IONPs to enter the brain. The treatment with LPA enhanced accumulation of IONPs in the brain as well as in the spleen (approximately 4-fold vs. control). Mice were injected intravenously with N-(trimethoxysilylpropyl) ethylenediaminetriacetate tri-sodium salt modified IONPs (EDT-IONPs) suspended in saline solution. For BBB disruption, LPA was injected along with the EDT-IONPs via the tail vein. Per the authors, transient modulation of the BBB by LPA achieved a significantly improved uptake of IONPs in brain parenchyma, while the treated mice revealed no sign of peripheral immune cell infiltration in the brain and no significant activation of microglia or astrocytes [100].

Although in the methods described above, the BBB was disrupted by different means (physical or chemical) to allow the crossing of large molecules, most of the passive methods try to take advantage of the impaired BBB that is common in pathological conditions. As mentioned earlier, in case of a brain tumor [101], EPR causes some “leakiness” of the BBB in tumor vasculature [102–104]. In one study [105] maghemite NPs were combined with a potential anticancer drug (caffeic acid). Following an intravenous injection of these NPs in mice bearing a U87 GBM, a negative contrast enhancement was specifically observed on MRI images in cancerous tissue, demonstrating a passive targeting of the tumor with these nanoplatforms.

In a different study [106], the potential applications of gold and SPION-loaded micelles (GSMs) coated by PEG-polycaprolactone (PEG-PCL) polymer for potential treatment and imaging of GBM were investigated relying on the EPR effect to deliver the micelles into the tumor. MRI-based visualization revealed an accumulation of GSMs in both the heterotopic flank and orthotopic brain GBM tumors and provided reliable hypointense MRI contrast

enhancement with good delineation of tumor borders. However, a disadvantage of using these brain tumor delivery methods is that they do not provide analytic information about the type of brain cancer.

3.1.2. Methods using active targeting mechanisms—For years, peptides, antibodies and small molecules have been used as free or as NP-attached ligands to facilitate transport to the brain [88,107–110]. In receptor-mediated endocytosis, such ligands bind to specific receptors on the surface of vascular EC layers and are internalized [111]. When the ligand/receptor complex is internalized and then released on the opposite side into the parenchyma, the process is termed transcytosis. As an active targeting reaction, transcytosis can increase the quantity of the imaging/therapeutic agent in the parenchyma and thus improve its efficiency. Transcytosis enables transport across an intact BBB and could be important for treatment of a disease that is in its "nascent" stage of development.

Common receptors for BBB transcytosis are the TfR, the low density lipoprotein-1 receptor (LRP-1) and the insulin receptor [112]. The TfR [113] is expressed by brain capillary ECs and serves as receptor mediated transport of iron-bound transferrin through the BBB and into normal brain. In an example for iron transport coupled NPs, Ghadiri et al. [114] conjugated magnetite dextran-spermine coated NPs to transferrin and facilitated crossing of the BBB. LRP-1 [115] is a member of LDL receptor family that has been proven to carry ligands, such as amyloid precursor protein (APP) and importantly angiopep-2 conjugated drugs across the normal BBB and diseased brain [116–119]. The insulin receptor is responsible for the import of insulin and insulin derivatives into the normal brain [120].

A common targeting agent for drug delivery across the BBB is the tripeptide arginine-glycine-aspartic acid (RGD). It specifically binds $\alpha v\beta 3$ for internalization that is overexpressed on tumor neovascular ECs, and therefore facilitates BBB crossing via integrin-mediated transcytosis [121]. cRGD (cyclic "arginine-glycine-aspartate" [122]) peptides are preferred because the cyclic tripeptides are less prone to enzyme peptidolytic cleavage and have been extensively used to target NPs into gliomas and other tumors [123–126].

Boucher et al. [127] studied a functionalized MRI contrast agent produced in a single step from genetically modified magnetotactic bacteria *in vivo* for application in MR-based molecular imaging of brain tumors in a mouse model of GBM. The outer surface of the magnetosomes was decorated with the RGD peptide by genetically manipulating a *Magnetospirillum magneticum* AMB-1 strain. Data analysis revealed a specific enhancement of the tumor contrast on MR images when applying the RGD-labeled magnetosomes compared to the unlabeled ones.

4. Imaging methods using IO formulations

4.1. MRI

The most commonly used magnetic imaging method is MRI. In this method, IO formulations are used as contrast agents. Image contrast may be weighted to demonstrate different anatomical structures or pathologies. Hydrogen protons of water molecules inside

imaged tissue return to their equilibrium states after a magnetic field induced orientation of their nuclear magnetic spins. This reorientation follows independent processes characterized by T1 (spin-lattice) and T2 (spin-spin) relaxation times.

IO species are commonly used as a T2 (or T2*) contrast agent, that means negative contrasts which change the T2 relaxation rate. Plots of relaxation rates 1/T2 and 1/T1 vs. Fe concentration are linear and exhibit characteristic slopes representing relaxivities r_2 and r_1. A high r_2^*/r_1 will indicate an excellent T2* contrast. For example, MRI r_2 and r_1 relaxivites of FDA approved contrasts are 98.3 and 23.9 mM^{-1} sec^{-1} for r_2 and r_1, respectively, in the case of Feridex (Endorem, ferumoxides) (particle size of 120–180 nm measured by photocorrelation spectroscopy), and 151.0 and 25.4 mM^{-1} sec^{-1}, respectively, for ferucarbotran (Resovist) [128].

To date, many known SPIONs have already exceeded these values. For example, cation-doped maghemite NPs [129] have reached relaxivity values of 522 (r_2^*) and 0.72 (r_1) mM^{-1} sec^{-1} and a ratio of 725 (r_2^*/r_1) as a result of testing different cation doping on the maghemite surface (size range of 6–7 nm measured by transmission electron microscopy [TEM]). In another study, cerium (Ce)-doped maghemite had an r_2^* of 189 and r_1 of 0.015 that raised the r_2^*/r_1 ratio to 12600, and PEI-grafted Ce-doped maghemite designed for gene delivery had an r_2^* of 168 mM^{-1} sec^{-1}, r_1 of 0.103 mM^{-1} sec^{-1} and r_2^*/r_1 ratio of 1631[24].

A nanocomposite with a diameter of 23.05 nm with hybrid character HSA_{DoE}/CAN-γ-Fe_2O_3 was prepared consisting of a human serum albumin (HSA) shell encapsulating a 6.6 nm Ce-doped maghemite CAN-γ-Fe_2O_3 [130]. For the composite, the relaxivity values were 482 (r_2^*) and 0.121 mM^{-1} sec^{-1} (r_1) and the r_2^*/r_1 ratio was 3983. Encapsulating the maghemite NPs within HSA improved the measured relaxivity due to a “clustering effect” of the SPIONs that were used.

An important factor for transverse relaxivity is the particle diameter. Due to the “clustering effect”, the magnetic NP diameter corresponds to the integral hydrodynamic diameter determined by dynamic light scattering (DLS), and not necessarily with a single particle diameter and therefore increased r_2^* values are measured [131].

The surface modification by cations uses defect-induced magnetism (DIM) [132] to influence the magnetism of the NPs, and subsequently, the relaxivity. Vacancies or defects introduced in any lattice-ordered structure can significantly affect and induce magnetism, due to changes in electron densities around any phase/defect/vacancy of such materials [133,134].

A 9.1 nm (by TEM) magnetite based composite with a polymer shell and RGD functionality that reached an r_2 value of 550.04 mM^{-1} sec^{-1} has been shown [135]. Another magnetite/polymersome nanocomposite [136] has reached an r_2 value of 611.6 mM^{-1} sec^{-1}, while albumin fabricated superparamagnetic iron oxide nanoparticles (uBSPIOs) [137] had values of r_2 = 444 mM^{-1} sec^{-1}, r_1 = 0.93 mM^{-1} sec^{-1} and r_2/r_1 = 478.

Even though IONPs are mainly used as negative (T2/T2*) contrast agents, several studies have been done to measure positive (T1) contrast [137–142]. An example of ultrasmall

ferrite NPs ($MnFe_2O_4$) [69] used as a positive contrast is shown in Fig. 3. In another recent study [143], zwitterion-coated very small SPIONs (ZES-SPIONs) were developed for a T1-weighted contrast-enhanced MRI as a potential alternative to Gd complexes to avoid long-term toxicity. To achieve this goal, the r_2/r_1 ratio had to be minimized while preserving a high value for r_1, similar to positive contrast agents.

The strategy of Wei et al. was to use maghemite NPs with a very small hydrodynamic diameter [143]. Maghemite was chosen because it is less magnetic than magnetite, and because the small diameter serves both relaxivity and a less toxic renal clearance. When ultrafine IONPs (uIONPs, 3.5 nm) with T1−T2 switchable MRI contrasts for tumor delivery were fabricated *in vivo* MRI revealed that the oligosaccharide coated uIONPs exhibited "bright" T1-contrast when dispersed in the tumor vasculature and peripheral area at 1 h after intravenous administration, followed by emerging "dark" T2 contrast in the tumor after 24 h [144]. The authors suggested that single-dispersed uIONPs in the bloodstream with T1 contrast self-assembled into larger clusters after residing inside the tumor and exhibited a favorable T2 contrast.

4.2. MPI

In addition to MRI which uses IONPs as a contrast agent to produce the MR signal, MPI uses the magnetic particle itself as the tracer and not as a contrast agent. It does so by utilizing an oscillating magnetic field to generate a signal derived from non-linear magnetization of the magnetic NPs [145]. The technology was first introduced in 2005 and is considered to be in pre-clinical use to date [146,147].

For this specific method, which is of great interest since it has a higher spatial resolution then MRI, the FDA approved ferucarbotran (Resovist) was usually used. In recent years, IONPs were studied extensively to be tailored to this type of imaging [145,148] and applied to research studies such as stem cell tracking [149]. One study utilized the high temporal resolution of MPI to assess aneurysm hemodynamics in a model [150] applying commercially available dextran coated magnetite NPs. In this study, where MRI and dynamic digital subtraction angiography (DSA) were used, the authors concluded that once MPI becomes clinically available, it may be a powerful tool for the same 4D analysis *in vivo* (a time-resolved 3D [time + 3D]) can be termed as 4D flow MPI or MRI). At present, however, the ability to acquire needed information by 4D MRI is not possible under *in vivo* conditions.

Another study used quantitative MPI to monitor transplantation, bio-distribution, and clearance of ferucarbotran-labelled human stem cells *in vivo* [151]. Ferucarbotran was also used by the same researchers to track the long-term fate of *in vivo* neural cell implants [152]. Ferucarbotran-labelled human stem cells were injected at three different locations in rat brains following a surgical procedure, with ferucarbotran/PBS used as a control. The animals were monitored for 87 days using a self-built MPI machine. To validate the findings, immunohistochemistry and MRI were used. Other than demonstrating longitudinal monitoring and quantifying implanted neural cell grafts, it was shown that the MPI signal was linear and could be used to quantify cell number *in vivo*. In addition, areas which were

inaccessible to optical, MRI and nuclear techniques (e.g., GI tract and pulmonary vasculature) could be managed by MPI.

4.3. Dual modality imaging

Other than focusing on only the two main techniques of MRI and MPI, many NPs with dual or multimodality [22,153,154] imaging methods were developed, combining MRI and/or MPI with optical imaging [155–157], sensitive and high resolution positron emission tomography (PET) [129,158], computed tomography (CT) [159] and other combinations, as the IO platform can be encapsulated, grafted and coated. For optical imaging, IONPs are usually grafted with a dye, more recently using near-infrared fluorescence (NIRF) such as cy 5.5 or similar dyes [160]. Also near-infrared (NIR) active polymers were introduced and used for coating [161].

As an example of such multimodality, an IO-based tri-modal nanoprobe for NIRF, photoacoustic tomography (PAT) and MRI was fabricated by Wu et al. [161]. PAT is based on the photoacoustic effect in which sound waves are formed following light absorption by an imaging reagent [162]. By using poly(isobutylene-alt-maleic anhydride) (PIMA) as the backbone, dopamine (Dopa) and IR-820 (indocyanine green analogue) were linked to produce a NIR-emitting multidentate polymer. The polymer was used to replace the oleate stabilizing molecule of the IONPs fabricated using the thermal decomposition method. As a proof of concept, the resulting IONPs@820-PIMA-Dopa which was found to be superparamagnetic and hydrophilic, was injected into healthy mice (distal, right anterior paw) for regional lymph node mapping using all three imaging methods – PAT, MRI and NIRF imaging.

In another study [163], an optically active semiconductor NP quantum dot (QD) with tunable fluorescence core, was encapsulated within a hollow paramagnetic IO shell as the T2 MRI contrast agent (r_2 of 304 mM^{-1} sec^{-1}). Another example that was reported [164], was the self-assembly of functionalized IONPs on the surface of molybdenum disulfide (MoS_2) nanosheets used to form a composite which was functionalized even further with PEG and PET enabling radioactive ^{64}Cu. Since MoS_2 sheets have high NIR absorbance, with the addition of SPIONs the composite could be used in photothermal therapy (PTT) as well as PAT, providing a triple modality MRI/PET/PAT imaging agent with PTT capabilities (Fig. 4). *In vivo* experiments for the composite in tumor bearing mice (intravenous injection) showed uptake in the tumor, as well as RES organs such as the liver. When image guided PTT treatment was utilized in tumor bearing mice (4T1 murine breast cancer), the tumor temperature increased to 51°C which resulted in the elimination of the tumor.

5. Treatment methods using IONPs

5.1. Temperature based treatment

As mentioned before, raising the temperature of a tumor may cause damage and even kill cancer cells. PTT usually requires activation of the agent using a laser, which limits the application to cancer types that are accessible by the laser. Magnetic NPs on the other hand, can cause temperature increase of a tissue by friction. The friction is due to movement of the

IONPs, and can be triggered by an external oscillating magnetic field coupled to radio frequency (RF), thus eliminating the need for a laser. Optimizing IONPs for this application is highly desirable [165–167].

For hyperthermia, specific absorption rate (SAR) values are used to evaluate the IONPs to measure the rate at which energy is absorbed by the sample when exposed to an RF electromagnetic field [168]. In an example of IONPs tailored for both MPI and magnetic hyperthermia, Zn was used to selectively dope magnetite NPs, both spherically and cubically shaped [169]. The doping alone enhanced the MPI signal by 2-fold, while adapting the field gradient used in MPI demonstrated focused magnetic hyperthermia heating. In addition, the Zn doped cubic NPs showed a 5-fold improvement in SAR values, over the non-doped spherical magnetite. Another strategy for amplifying the heating efficiency is by combining magnetic hyperthermia and photothermal treatment. In one study this was done by using magnetite nanocubes with an edge length of 20 nm [170]. Niculaes et al. [166] studied the heating efficiency under magnetic hyperthermia of individually coated IO (FeO/Fe_3O_4 core −shell) nanocubes versus soft colloidal nanoclusters consisting of small groupings of nanocubes arranged in different geometries. They showed that controlled grouping of NPs composed of two and three nanocubes increases SAR values, while conversely, forming centrosymmetric clusters having more than four nanocubes leads to lower SAR values. In addition, the annealing process (heat treatment), also improved SAR values.

5.2. Treatment that manipulates the immune system

Another form of treatment is to use NPs to polarize immune system cells [171]. In an example [67], ferumoxytol was shown to inhibit tumor growth by inducing pro-inflammatory macrophage polarization in tumor tissues. *In vitro*, macrophages exposed to ferumoxytol displayed increased mRNA associated with pro-inflammatory Th1-type responses. *In vivo*, ferumoxytol significantly inhibited growth of adenocarcinomas in mice. In addition, intravenous ferumoxytol treatment prior to intravenous tumor cell inoculation prevented the development of liver metastases. Furthermore, the observed tumor growth inhibition was accompanied by increased presence of pro-inflammatory M1 macrophages in the tumor tissues. In the CNS however, such an approach may be problematic, due to a very low number of macrophages in the brain (usually termed as “infiltrating” or “migrating” macrophages since the brain resident “macrophage-like” cells are the microglia cells), so even though it is still unknown if there are enough macrophages in the brain to facilitate an effective treatment, some research is still being done in this area.

Another interesting approach which was reported recently, is utilizing the natural ability of monocytes and monocyte-derived macrophages (MDMs) to uptake micro- and nano-size particles (IO in particular), allowing easy loading of small molecular agents onto the “cell carriers” [172]. Since these cells can traverse tissue barriers and traffic into damaged sites caused by inflammation, infection, and tissue degeneration, they are attractive candidates for drug carriage and gene delivery. SPIONs were chosen for this study because of the multiple roles they could be applied to in cell-based drug delivery studies. The authors identified SPIONs with 30 nm core size and oleic acid plus amphiphilic polymer coats (“SHP30”) to have the most efficient MDM uptake accompanied with the lowest cytotoxic effects [172]. *In*

vivo, an acute brain encephalitis mouse model (inflammation induced by intracranial [IC] injection of bacterial lipopolysaccharide, LPS) was used. Twenty-four hours post trigger injection, control or SHP30 loaded MDM were introduced into recipient animals by intravenous adoptive transfer. Histological analysis confirmed that at 48 h post cell intravenous infusion, both control and SHP30 carriage donor cells appeared in the brain and staining of astrocytes revealed these recruited donor cells had accumulated in the inflamed region of the brain. Prussian blue staining (specific for iron) validated the presence of SHP30 in the carrier cell cytoplasm [172].

5.3. Cell based therapy and nucleic acid delivery

Since IONPs can be imaged, monitored and quantified by methods including TEM, wet chemical iron assays, inductively coupled plasma (ICP) and conventional staining of fluorescence labeled NPs, the magnetic biological targeting and the delivery of nucleic acids into cells (transfection) render this class of NPs a very strong modality for cell therapy [149,173–175]. The systemic or direct delivery of nucleic acids (DNA; all kinds of RNA including siRNA, microRNA; antisense oligonucleotides [AON]) offers attractive ways of delivery to CNS targets to even promote noninvasive treatment [65,176–184].

Recently, transdifferentiation (TD)-derived neural stem cells (iNSCs) were shown to be an efficacious therapeutic alternative for the treatment of brain cancer [185]. The genetically engineered iNSCs equipped with optical reporters and tumoricidal gene product retain the capacity to differentiate cells and induce apoptosis in co-cultured human GBM cells. Time-lapse imaging showed that iNSCs are tumoritropic, homing rapidly to co-cultured GBM cells and migrating extensively to dispersed distant tumor foci in the murine brain. iNSC delivery of the anticancer molecule TRAIL decreased the growth of established solid and diffuse patient-derived orthotopic GBM xenografts and significantly prolonged the median survival of mice. These findings establish a strategy for creating autologous cell-based therapies to treat patients with aggressive forms of brain cancer.

An example of an IO-neural stem cell transfection agent can be seen in the work of Adams et. al. [175], where researchers used PEI-grafted maghemite NPs combined with magnetofection to increase DNA transfection of neuronal stem cells. Neuronal stem cells are usually very difficult to transfect. The main challenge in this type of delivery, was that the nucleic acid load needed to be released in the cell cytoplasm. PEI (a cationic polymer) is used to open the endosome membrane by activating the “proton sponge” effect. These complexes however, could not penetrate into the brain [186–189].

Another interesting application, was the use of IO to label human mesenchymal stem cells, which in turn, released exosomes that contained IO. Furthermore, these exosomes were efficiently endocytosed by tumor cells. Exosomes from Venofer-labeled cells expressing the yCD::UPRT gene in the presence of the prodrug 5-fluorocytosine inhibited tumor growth in a dose-dependent fashion when PC3 and HeLa cell lines were tested. On the other hand, a partial killing effect of alternating magnetic field (AMF) exposure under the same conditions was observed with the human glioma cell line U118. Human primary GBM and recurrent astrocytoma cells treated with NPs from yCD::UPRT-DP-MSCs/Fe and exposed to an AMF

differed in the sensitivity to hyperthermia-induced cell death. While most GBM cells died within 5 days after AMF, the remainder died during subsequent days [190].

6. Recent examples of imaging and treatment of brain tumors using IONPs

Multiple examples can be found for the utilization of IONPs for imaging and treatment of brain tumors [64,191–199] (Table 1). IONPs, coated with the tumor-penetrating peptide iRGD reduced experimental breast cancer metastasis and strongly inhibited tumor progression in the brain when applied in the early stages of metastasis development [200]. In this case, anti-metastatic activities of the iRGD peptide and the combined action of the iron particles were the suggested mechanism. While IO on the surface of NPs can modulate the bioavailability, biodistribution, and pharmacokinetic characteristics of payload therapeutics they might also prolong the half-life of the presented peptides in the circulation.

PEGylated magnetic IONPs were synthesized with the aim of providing proof of concept results for the remote cancer cell killing by magnetic fluid hyperthermia [201]. The interaction of the PEGylated IONPs with a U87 GBM cell line was studied and highlighted the superior efficiency of multicore (nanoflowers) vs. monocore (nanospheres) IONPs for magnetic hyperthermia, leading to 80% cancer cell death in medically translatable conditions.

In a different study, composite iron oxide-gadolinium-containing Prussian Blue (Fe_3O_4@GdPB) NPs were presented as a theranostic agent for T1-weighted (T1W) MRI and PTT of tumors. A murine neuro-blastoma model was used. Per the authors, the NPs possessed the ability to function as effective contrast agents in both T1W and T2W scans as well as effective PTT agents [202].

Magnetic-fluid-loaded liposomes (MFLs) were developed with a hydrodynamic diameter of 212 ± 29 nm by the entrapment of superparamagnetic maghemite nanocrystals in submicronic PEGylated rhodamine-labelled phospholipid vesicles [203]. The strategies for using MFLs were both selective magnetic targeting of malignant tumors localized in brain and non-invasive traceability by MRI. As assessed by *in vivo* 7-T MRI and *ex vivo* electron spin resonance, 4-h exposure to a magnetic field gradient efficiently concentrated MFLs into human U87 GBMs implanted in the striatum of mice. The magnetoliposomes were then retained as checked by MRI monitoring over a 24-h period. The magnetic field gradient emphasized MFL distribution solely in the tumor according to the EPR effect, while comparatively very low amounts were recovered in the other cerebral areas.

In a different study, an integrated liposome was used that simultaneously combined multiple-imaging agents such as SPIONs and QDs for optical imaging as well as therapeutic drug [8]. The drug, Cilengitide (CGT), is a cyclic arginine–glycine–aspartic pentapeptide antagonist that inhibits overexpression of integrin receptors on GBM and tumor-associated capillary ECs. Moreover, an additional method such as a combination of low-intensity ultrasound with microbubbles, referred to as ultrasound-targeted microbubble destruction (UTMD), was used to enhance the transportation of therapeutics across the BBB without causing damage to the

brain. A focused ultrasound (FUS) emitter however, usually intracranial [204], or alternatively a linear array transducer, was placed on the skull. The resulting nano system was aimed for glioma-targeted delivery of its loading cargo under an exogenous magnetic field. The resulting NPs exhibited a diameter of 100 ± 1.24 nm, zeta potential of −17.10 ±0.11 mV, and an r_2 value of 172.6 mm^{-1} s^{-1}. The specific distribution of the system in glioma produced a negative-contrast enhancement effect on glioma by MRI and also made the tumor zone emit strong fluorescence under magnetic targeting (MT). In addition, the ability of the liposomes to guide the accurate resection of glioma was confirmed by surgery. Finally, *in vivo* inhibition of tumors was confirmed after intravenous injection of liposomes under MT.

One advantage in encapsulating unstable agents in microbubbles is to prevent fast degradation, while reducing the required dose [204]. Also, the encapsulated agents can be control-released during the FUS-triggered microbubble destruction process, thereby reducing the off-target dose. In this study, the authors reported the fabrication of a therapeutic complex in which SPIONs are directly conjugated with doxorubicin and are embedded in lipid microbubbles.

A recent example of the development of IONPs is the targeted T1-weighted MR imaging of glioma using Fe_3O_4 NPs conjugated with PEG-linked RGD [205].

A contrast agent comprised of two FDA approved components, indocyanine green (ICG) and SPIONs in the absence of amphiphilic or carrier materials to enable preoperative detection by MRI and intraoperative photoacoustic (PA) imaging was also developed [206]. ICG–SPIONs clusters are stable in physiologic conditions, can be taken up by tumors via passive targeting (i.e., EPR), and are detectable by MR. In a preclinical surgical resection mouse model, following the injection of the clusters animals undergoing PA-guided surgery demonstrated increased progression-free survival compared to animals undergoing surgery under the microscope.

Tumor-associated macrophages that contained IONPs coated with near-infrared fluorescent silica as guidance during the surgery of orthotopic xenografts were also targeted [207]. Abundant macrophage infiltration is a key feature of GBM margins, and it is well associated with poor prognosis. The authors synthesized the fluorescent silica coated iron oxide nanoparticles (NF-SIONs) of 37 nm size to maximize macrophage uptake by endocytosis. The NF-SIONs selectively visualized tumor-associated macrophage populations by *in vitro* magnetic imaging of living cells as well as by *in vivo* fluorescence imaging. In the orthotopic GBM xenograft models, the NF-SIONs could penetrate the BBB and specifically delineate the tumor.

MRI tracking of PEG-coated superparamagnetic IO-labelled placenta derived mesenchymal stem cells (MSCs) mimicking GBM stem-like cells in a mouse model was also demonstrated [208]. MSCs can display homing and infiltration properties towards tumor cells and, therefore, are considered to be a promising cellular targeting vector for brain tumor therapy. However, they are limited to local-regional delivery in current preclinical models. In the current study, researchers investigated whether placenta-derived MSCs (P-MSCs) are a

superior cellular vector for systemic targeting of GBM stem-like cells (GSCs). Results demonstrated that P-MSCs had greater migratory activity similar to GSCs and across the BBB in comparison with bone marrow-derived MSCs. In addition, chemokine ligand 5 was identified as a chemoattractant responsible for the GBM tropism of P-MSCs. PEG–-SPIONs were synthesized for cellular labelling and imaging P-MSCs, displaying high cellular uptake and no cytotoxic effect on P-MSC cell proliferation or stemness property. The homing effects of intravenously administered PEG–SPIO-labelled P-MSCs towards intracerebral GSCs were able to be detected in mice models through MRI, supporting the possibility of systemic P-MSC based cell therapy for aggressive GSCs.

In addition to these studies, a study was performed to evaluate the potential of vascular cell adhesion molecule 1 (VCAM-1)-targeted MRI for early detection of brain micrometastases [209]. The study included mouse models across multiple primary tumor types. All models showed disseminated micrometastases in the brain, together with endothelial VCAM-1 upregulation. T2-weighted MRI of tumor-bearing mice injected with VCAM-1 targeted iron oxide microparticles (VCAM-MPIO) showed increased signal intensities compared to control cohorts, and without BBB impairment.

Exosomes were loaded with SPIONs and curcumin (Cur) and the exosome membrane was conjugated with neuropilin-1-targeted peptide (RGERPPR, RGE) by click chemistry [210]. When administered to glioma cells (U 251) and orthotopic glioma models, they found that these engineered exosomes could cross the BBB, with results for targeted imaging and therapy of glioma that were good. Furthermore, SPION-mediated magnetic flow hyperthermia and Cur-mediated therapy also showed a potent synergistic antitumor effect.

An example of the use of IO in human patients can be seen in a retrospective study analyzing MRI results [211]. The authors analyzed ferumoxytol and gadolinium contrast enhanced T1-weighted 3T MRI in 45 patients with GBM over multiple clinical timepoints. They observed a significantly elevated mismatch ratio compared with disease recurrence within tumor-IDH-1 wild-type patients. Patients positive for the mutation demonstrated a significantly reduced mismatch ratio with the development of pseudoprogression compared with the ratio for disease recurrence. The authors suggested that ferumoxytol to gadolinium contrast mismatch ratios are an MRI biomarker for the diagnosis of pseudoprogression in patients with GBM. In a different study in human patients, ferumoxytol-enhanced MRI was used as a noninvasive imaging biomarker of macrophages in adults with high-grade gliomas [212]. It was shown that the results of MRI measurements obtained after ferumoxytol administration correlated with the content of iron-containing macrophages.

Although in most studies MRI was widely used [213], there are also examples of the application of MPI. For example, monodisperse IONPs with median core diameters ranging from 14 to 26 nm were fabricated [214]. Their surfaces were conjugated with lactoferrin to convert them into brain glioma targeting agents. The lactoferrin-conjugated IONPs showed specific cellular internalization into C6 glioma tumor cells with a 5-fold increase in the magnetic particle spectroscopy signal which was used to evaluate MPI capability, compared to IONPs without lactoferrin, both after 24 h of incubation.

Recently, the advantage of using IONPs in combination with radiotherapy was also demonstrated [215]. In this study, six recurrent GBM patients were treated with intracavitary thermotherapy after coating the resection cavity wall with SPIONs.

In a preclinical study, the repolarization of myeloid derived suppressor cells (MDSCs) via magnetic NPs promoted radiotherapy in glioma [216]. The $Zn_{0.4}Fe_{2.6}O_4$ based magnetic nanoplatform (Fig. 5) was modified with di-mercaptosuccinic acid (DMSA) and the cationic polymer PEI (Fig. 5A). Seven days post tumor implantation, mice were treated with PBS or 25 μg NPs (Fig. 5B). The heads of mice were exposed to 2 Gy of radiation each day for 4 days (total 8 Gy). Two glioma models (CT-2A, U87) were used. As shown in Fig. 5C, radiotherapy or NP monotherapy presented marginally prolonged median survival of the CT-2A model (a shift from 25 to 30 days). In contrast, the NP with radiotherapy combination considerably extended median survival to 38 days, which was a 50% prolongation of survival. The U-87 MG xenograft model was also implanted in immunodeficient nude mice (Fig. 5D). While both of the radiotherapy and NPs groups showed no significant difference in median survival compared with the PBS group, the radiotherapy and NP combination resulted in a 45-day median survival, which was significant longer compared with the 34 days of the control. Furthermore, it was shown that in addition to tumor cell death induced by NP-mediated radiotherapy, the recruitment and regulation of MDSCs (a heterogeneous population within the tumor microenvironment of immature myeloid derived cells) resulted in another synergistic effect further prolonging the survival of glioma-bearing mice. Basically, NPs with radiation treatment served as a local stimulator for re-educating MDSCs to attack tumor cells and through inflammatory polarization this pro-inflammatory function further enhanced radio-therapeutic effects.

7. Biosafety of IONPs in the brain

To date, numerous studies have investigated the biocompatibility and potential toxicity of IONPs both in the clinic and using experimental models [215,217–219]. IO biosafety can be influenced by multiple factors. The above-mentioned oxidation state and crystalline structure (maghemite γ-Fe_2O_3 vs. magnetite Fe_3O_4) is one example of an important factor, while surface functionalization and decoration are another. Since IO toxic effects on cells and tissues is in part caused by iron-mediated radical formation and oxidative stress, the Fe oxidative state can be very important [220]. Recently, the absence of cytotoxicity towards microglia was demonstrated for IO (α-Fe_2O_3, hematite [221]) nano-rhombohedral (N-Rhomb) [222]. Per this study internalization of rhodamine b labeled-α-Fe_2O_3 N-Rhomb by microglia in the mouse brain was observed, and a dose-dependent increase in the cellular iron content as probed by cellular fluorescence was measured in cultured microglia after NP exposure. The cells maintained clear viability, exhibiting little to no cytotoxic effects after 24 and 48 h at acceptable, physiological concentrations. Importantly, the NP exposure did not induce microglial cells to produce either tumor necrosis factor alpha (TNFα) nor interleukin 1-beta (IL1β), two pro-inflammatory cytokines, nor did the exposure induce the production of nitrites and reactive oxygen species (ROS), which are common indicators for the onset of inflammation [222]. An earlier study revealed that ferucarbotran NPs suppress the production of IL1β via the secretory lysosomal pathway in murine microglial cells [223]. In another study magnetite (Fe_3O_4) was investigated [224], demonstrating cytotoxicity and

proliferative impairment induced in human brain cell cultures after short- and long-term exposure to magnetite NPs. For two representative cell types of human CNS in culture (D384 astrocytes and SH-SY5Y neurons) it was shown that Fe_3O_4 NPs can accumulate in astrocytes in a concentration-and time-dependent manner, and functions of mitochondria could be affected at the cellular level. Nevertheless, the cellular membrane of astrocytes was not altered by Fe_3O_4 NPs within 48 h of exposure. SH-SY5Y neurons were less susceptible to magnetite NPs after either shortor long-term exposure [224]. In an older study, it was demonstrated that partial oxidation of nano-sized zerovalent iron in magnetite/maghemite as well as surface modifications, for example by reaction with sodium polyaspartate, decreased neurotoxicity [225]. Cation doped maghemite NPs were also studied extensively for having toxic effects both *in vivo* and *in vitro* in cells types such as Su86.86, T3M4, PDAC, HCT116, HT29 colon carcinoma, U87MG, A172, T98G-GBM, and NB1, SK-N-5Y, SK-N-BE2-neuroblastoma cells. No toxic effects were seen [129].

In addition to crystal structure and oxidation state, the surface grafting can also induce toxicity, since the surface coating/ligands come in direct contact with the biological system. In one example, magnetite particles coated with different natural amino acids (Gly, Lys, Arg, Phe and Tys) were studied, and toxicity was tested on HFF2 cell lines. Per the authors, MTT assay did not indicate growth inhibition [218]. IONPs were coated with an amphiphilic polymer and PEGylated, while cultured human endothelial cells (HUVEC) and murine macrophages were used as models for cells exposed to systemic administration of NPs. The pegylated NPs exhibited no cytotoxicity or inflammatory responses while the non-PEGylated NPs showed a concentration-dependent increase of cytotoxicity and of TNFα production by macrophages, and nitric oxide production by HUVECs. Cell uptake analysis suggested that after PEGylation, the NPs were less internalized by macrophages or by HUVECs. These results suggest that the choice of the polymer and the chemistry of surface functionalization are crucial features for conferring IONP biocompatibility [226].

Recently, PEG coated magnetite NP biokinetics were evaluated in mice and nonhuman primates. It was demonstrated that pharmacokinetics is similar in mice (nude athymic) and macaques in the blood, liver, spleen, and muscle, but differ in kidneys, brain, and bone marrow. It was demonstrated that full-body MRI is practical, rapid, and cost-effective for tracking NPs noninvasively with high spatiotemporal resolution [227].

Information on the interaction of IONPs with different brain regions and cells can be found [220,228]. For example, one study focused on the mechanisms involved in IONP-induced microglial toxicity [229]. Per this study, rapid iron liberation from IONPs at acidic pH and ironcatalyzed ROS generation are involved in the IONP-induced toxicity of microglia and suggest that the degree of resistance observed for astrocytes and neurons against acute IONP toxicity is a consequence of a relatively slow mobilization of iron from IONPs during lysosomal degradation [229].

The basic science studies discussed above are active and clinical trial usage has also begun. The phase-I clinical study results of combined intracavitary thermotherapy with IONPs and radiotherapy as a local treatment modality in six recurrent GBM patients was briefly mentioned above [215]. In this study, the GBM patients were treated with intracavitary

thermotherapy after coating the resection cavity with superparamagnetic IONPs. Patients underwent six 1-h hyperthermia sessions in an AMF and received concurrent fractionated radiotherapy at a dose of 39.6 Gy. The applied commercial magnetic fluid MFL AS-1 (NanoTherm®) consisted of an aqueous dispersion of SPIONs with an iron concentration of 112 mg/ml. The NPs have magnetite (Fe_3O_4) cores of approximately 12 nm diameter coated with aminosilane, a bioinert, enzymatically uncleavable silicium compound with a positively charged surface that provokes fast adsorption to negatively loaded tissue proteins. Although there were no major side effects during active treatment, after 2–5 months patients developed an increasing number of clinical symptoms. Histopathology revealed sustained necrosis directly adjacent to aggregated NPs without evidence for tumor activity. Immunohistochemistry showed upregulation of caspase-3 and heat shock protein 70, in addition to prominent infiltration of macrophages with ingested NPs and CD3+ T-cells. Flow cytometric analysis of freshly prepared tumor cell suspensions revealed increased intracellular ratios of IFN-γ over IL-4 in CD4+ and CD8+ cells. Further analysis indicated memory T cells, activation of tumor-associated myeloid cells and microglia with upregulation of HLA-DR and PD-L1. The authors concluded that intracavitary thermotherapy combined with radiotherapy can induce a prominent inflammatory reaction around the resection cavity which might trigger potent antitumor immune responses possibly leading to long-term stabilization of recurrent GBM patients.

Finally, the long-term metabolism and clearance of IONPs from the brain over time also needs to be taken in account. In an earlier study [191], Iron oxide nanoparticles (clinical ferumoxtran-10, ferumoxides, and ferumoxytol) were administered in normal rats by intracerebral inoculation or intraarterially using osmotic blood-brain barrier opening, and intravenously in nude rats with intracerebral tumor xenografts. Rat brains were imaged by MRI at multiple time points and were then assessed for iron histochemistry and pathological features. In normal rats, after intracerebral injection, MRI signal changes declined slowly over weeks to months. After trans-vascular delivery, only transient (3 days) enhancement was seen with ferumoxtran-10 and ferumoxytol, whereas ferumoxides induced long-term (28 days) signal dropout. No pathological brain cell or myelin changes were detected after delivery of the agents to normal brains. In tumor bearing rat models, ferumoxtran-10 enhanced one small-cell lung carcinoma intracerebral tumor, which correlated with iron staining in cells with macrophage morphological features at the tumor margin. That data suggests that intracellular trapping by reactive cells such as astrocytes and macrophages is a contributing factor towards signal enhancement in brain tumors.

Other studies which investigated the metabolism of IONPs, shed more light on the relevant mechanisms of degradation [221,230–232]. In a similar manner to other cell types, the cells of the brain internalize IONPs by endocytosis which leads to the presence of IONPs in intracellular vesicles. Depending on the given cell, the IONP-containing vesicles are then directed to the lysosomal compartment where iron is liberated from IONPs due to acidic environments in these organelles. Ferrous ions are then transported into the cytosol by the divalent metal transporter 1 (DMT1). In the cytosol, iron ions may be used by the cell for the synthesis of iron-containing proteins. They may also be exported outside of the cell or induce the synthesis of the iron storage protein ferritin. It can also catalyze the generation of reactive oxygen species (ROS) using Fenton chemistry. Interestingly, one study describes a

model in which a reservoir of intact nanoparticles coexists along with the rapidly degraded nanocrystals [231]. However, these results were only obtained in a 20 mM acidic citric medium and not *in vitro* or *in vivo*.

8. Conclusions, future directions and outlook

IONPs are widely used in the clinic for diagnostic/prognostic purposes, especially MRI, as well as for treatment of diseases such as anemia. In this review we discussed the current usage of IONPs and described new directions for their future clinical applications that include imaging and treatment of brain tumors (Fig. 6). The ability to use IONPs for magnetic tumor targeting (Fig. 6) and their diversity make them attractive NPs for these future applications. The capability of IONPs to effectively cross the BBB while targeting brain cells and disease-derived macromolecular structures have moved IONPs to the forefront of applications.

In the field of imaging, two promising main advancements were shown: the preclinical MPI which is the latest new imaging method to be developed, as well as the use of IO as a positive contrast in MRI. Additionally, the potential of IONPs to be used for treatment using hyperthermia and polarization of immune cell phenotype also holds promise for the future. Hyperthermia, immune response, externally controlled movement in combination with magnetism and structural design are open areas for creative new applications. However, the combination of imaging, targeting and therapy using one nanosystem is the most promising direction of all.

It is anticipated that additional magnetic IONP formulations will be developed and used in the near future, especially for organs that are not easily accessible such as the brain, and other internal organs such as the lungs and liver. Delivery of MRI/MPI agents might also become useful in other brain pathological conditions such as Alzheimer's and Parkinson's diseases. Although the biosafety issue is still not resolved, it has been shown that controlling properties of the IONPs such as oxidation state and surface functionalities can address some of the concerns, thereby increasing the potential of IO-based NPs to be used in biomedicine in general, and in neurosciences specifically.

Acknowledgments

This work was supported by the following grants: NIH R01 CA188743, NIH/NCI R01CA206220, NIH/NCI 1R01 CA 209921-01 and NIH/NCI R01 CA230858-01.

References

[1]. Ballabh P, Braun A, Nedergaard M, The blood–brain barrier: an overview: structure, regulation, and clinical implications, Neurobiol. Dis 16 (2004) 1–13, 10.1016/j.nbd.2003.12.016. [PubMed: 15207256]

[2]. Marcos-Contreras OA, de Lizarrondo SM, Bardou I, Orset C, Pruvost M, Anfray A, Frigout Y, Hommet Y, Lebouvier L, Montaner J, Hyperfibrinolysis increases blood–brain barrier permeability by a plasmin-and bradykinin-dependent mechanism, Blood 128 (2016) 2423–2434, 10.1182/blood-2016-03-705384. [PubMed: 27531677]

[3]. McDannold N, Vykhodtseva N, Hynynen K, Blood-brain barrier disruption induced by focused ultrasound and circulating preformed microbubbles appears to be characterized by the

mechanical index, Ultrasound Med. Biol 34 (2008) 834–840, 10.1016/j.ultrasmedbio.2007.10.016. [PubMed: 18207311]

[4]. Wiley DT, Webster P, Gale A, Davis ME, Transcytosis and brain uptake of transferrin-containing nanoparticles by tuning avidity to transferrin receptor, Proc. Natl. Acad. Sci 110 (2013) 8662–8667, 10.1073/pnas.1307152110. [PubMed: 23650374]

[5]. Paris-Robidas S, Emond V, Tremblay C, Soulet D, Calon F, In vivo labeling of brain capillary endothelial cells after intravenous injection of monoclonal antibodies targeting the transferrin receptor, Mol. Pharmacol 80 (2011) 32–39, 10.1124/mol.111.071027. [PubMed: 21454448]

[6]. Louis DN, Ohgaki H, Wiestler OD, Cavenee WK, Burger PC, Jouvet A, Scheithauer BW, Kleihues P, The 2007 WHO classification of tumours of the central nervous system, Acta Neuropathol. 114 (2007) 97–109, 10.1007/s00401-007-0278-6. [PubMed: 17618441]

[7]. Alifieris C, Trafalis DT, Glioblastoma multiforme: pathogenesis and treatment, Pharmacol. Ther 152 (2015) 63–82, 10.1016/j.pharmthera.2015.05.005. [PubMed: 25944528]

[8]. Xu HL, Yang JJ, ZhuGe DL, Lin MT, Zhu QY, Jin BH, Tong MQ, Shen BX, Xiao J, Zhao YZ, Glioma-targeted delivery of a theranostic liposome integrated with quantum dots, superparamagnetic iron oxide, and cilengitide for dual-imaging guiding cancer surgery, Adv. Healthc. Mater 7 (2018) 1701130, , 10.1002/adhm.201701130.

[9]. Van Meir EG, Hadjipanayis CG, Norden AD, Shu HK, Wen PY, Olson JJ, Exciting new advances in neuro-oncology: the avenue to a cure for malignant glioma, CA Cancer J. Clin 60 (2010) 166–193, 10.3322/caac.20069. [PubMed: 20445000]

[10]. Rizvi S, Asghar AH, Mehboob J, Gliosarcoma: a rare variant of glioblastoma multiforme, J. Pak. Med. Assoc 60 (2010) 773–775. [PubMed: 21381591]

[11]. DeAngelis LM, Brain tumors N Engl. J. Med 344 (2001) 114–123, 10.1056/NEJM200101113440207.

[12]. Hehr T, Budach W, Lamprecht U, Belka C, Classen J, Trubenbach J, Wehrmann M, Dietz K, Bamberg M, Experimental thermoradiotherapy in malignant hepatocellular carcinoma, Int. J. Radiat. Oncol. Biol. Phys 55 (2003) 1374–1380, 10.1016/S0360-3016(02)04615-1. [PubMed: 12654450]

[13]. Hehr T, Wust P, Bamberg M, Budach W, Current and potential role of thermoradiotherapy for solid tumours, Onkologie 26 (2003) 295–302, 10.1159/000071628. [PubMed: 12845217]

[14]. Charles NA, Holland EC, Gilbertson R, Glass R, Kettenmann H, The brain tumor microenvironment, Glia 59 (2011) 1169–1180, 10.1002/glia.21136. [PubMed: 21446047]

[15]. Jackson C, Ruzevick J, Phallen J, Belcaid Z, Lim M, Challenges in immunotherapy presented by the glioblastoma multiforme microenvironment, Clin. Dev. Immunol 2011 (2011), 10.1155/2011/732413.

[16]. Sudhakar A, History of cancer, ancient and modern treatment methods, J. Cancer Sci. Therapy 1 (2009) 1–4, 10.4172/1948-5956.100000e2.

[17]. Witteles RM, Fowler MB, Telli ML, Chemotherapy-associated cardiotoxicity: how often does it really occur and how can it be prevented? Heart Fail. Clin 7 (2011) 333–344, 10.1016/j.hfc.2011.03.005. [PubMed: 21749885]

[18]. Manjili MH, The inherent premise of immunotherapy for cancer dormancy, Cancer Res. 74 (2014) 6745–6749, 10.1158/0008-5472.CAN-14-2440. [PubMed: 25411346]

[19]. Sun X, Su S, Chen C, Han F, Zhao C, Xiao W, Deng X, Huang S, Lin C, Lu T, Long-term outcomes of intensity-modulated radiotherapy for 868 patients with nasopharyngeal carcinoma: an analysis of survival and treatment toxicities, Radiother. Oncol 110 (2014) 398–403, 10.1016/j.radonc.2013.10.020. [PubMed: 24231245]

[20]. Tsai M-F, Hsu C, Yeh C-S, Hsiao Y-J, Su C-H, Wang L-F, Tuning the distance of rattle-shaped IONP@shell-in-shell nanoparticles for magnetically-targeted photothermal therapy in the second near-infrared window, ACS Appl. Mater. Interfaces 10 (2018) 1508–1519, 10.1021/acsami.7b14593. [PubMed: 29200260]

[21]. Monaco I, Arena F, Biffi S, Locatelli E, Bortot B, La Cava F, Marini GM,Severini GM, Terreno E, Comes Franchini M, Synthesis of lipophilic core–shell Fe3O4@SiO2@Au nanoparticles and polymeric entrapment into nanomicelles: a novel nanosystem for in vivo active targeting and

magnetic resonance–photoacoustic dual imaging, Bioconjug. Chem 28 (2017) 1382–1390, 10.1021/acs.bioconjchem.7b00076. [PubMed: 28453929]

[22]. Lee N, Yoo D, Ling D, Cho MH, Hyeon T, Cheon J, Iron oxide based nanoparticles for multimodal imaging and magnetoresponsive therapy, Chem. Rev 115 (2015) 10637–10689, 10.1021/acs.chemrev.5b00112. [PubMed: 26250431]

[23]. Thomsen LB, Thomsen MS, Moos T, Targeted drug delivery to the brain using magnetic nanoparticles, Ther. Deliv 6 (2015) 1145–1155, 10.4155/tde.15.56. [PubMed: 26446407]

[24]. Israel LL, Lellouche E, Kenett R, Green O, Michaeli S, Lellouche JP, Ce3/4+ Cation-functionalized maghemite nanoparticles towards siRNA-mediated gene silencing, J. Mater. Chem. B 2 (2014) 6215–6225, 10.1039/C4TB00634H. [PubMed: 32262139]

[25]. Israel L, Lellouche E, Grenèche J, Bechor M, Michaeli S, Ultrasound-mediated surface engineering of theranostic magnetic nanoparticles: an effective one-pot functionalization process using mixed polymers for siRNA delivery, J. Nanomed. Nanotechnol 7 (2016) 2, 10.4172/2157-7439.1000385.

[26]. Huber DL, Synthesis, properties, and applications of iron nanoparticles, Small 1 (2005) 482–501, 10.1002/smll.200500006. [PubMed: 17193474]

[27]. Ling D, Hyeon T, Chemical design of biocompatible iron oxide nanoparticles for medical applications, Small 9 (2013) 1450–1466, 10.1002/smll.201202111. [PubMed: 23233377]

[28]. Gupta AK, Gupta M, Synthesis and surface engineering of iron oxide nanoparticles for biomedical applications, Biomaterials 26 (2005) 3995–4021, 10.1016/j.biomaterials.2004.10.012. [PubMed: 15626447]

[29]. Cornell RM, Schwertmann U, The Iron Oxides: Structure, Properties, Reactions, Occurrences and Uses, John Wiley & Sons, 2003.

[30]. Jolivet JP, Chanéac C, Tronc E, Iron oxide chemistry. From molecular clusters to extended solid networks, Chem. Commun (2004) 477–483, 10.1039/B304532N.

[31]. Massart R, Dubois E, Cabuil V, Hasmonay E, Preparation and properties of monodisperse magnetic fluids, J. Magn. Magn. Mater 149 (1995) 1–5, 10.1016/0304-8853(95)00316-9.

[32]. Schwertmann U, Cornell RM, Iron Oxides in the Laboratory: Preparation and Characterization, John Wiley & Sons, 2008.

[33]. Mathew DS, Juang RS, An overview of the structure and magnetism of spinel ferrite nanoparticles and their synthesis in microemulsions, Chem. Eng. J 129 (2007) 51–65, 10.1016/j.cej.2006.11.001.

[34]. Morales M, Bomati-Miguel O, Pérez de Alejo R, Ruiz-Cabello J, Veintemillas-Verdaguer S, O'Grady K, Contrast agents for MRI based on iron oxide nanoparticles prepared by laser pyrolysis, J. Magn. Magn. Mater 266 (2003) 102–109, 10.1016/S0304-8853(03)00461-X.

[35]. Maity D, Kale S, Kaul-Ghanekar R, Xue J-M, Ding J, Studies of magnetite nanoparticles synthesized by thermal decomposition of iron (III) acetylacetonate in tri (ethylene glycol), J. Magn. Magn. Mater 321 (2009) 3093–3098, 10.1016/j.jmmm.2009.05.020.

[36]. de Tercero MD, Bruns M, Martínez IG, Türk M, Fehrenbacher U, Jennewein S, Barner L, Continuous hydrothermal synthesis of in situ functionalized iron oxide nanoparticles: a general strategy to produce metal oxide nanoparticles with clickable anchors, Part. Part. Syst. Charact 30 (2013) 229–234, 10.1002/ppsc.201200109.

[37]. Roca A, Morales M, Serna C, Synthesis of monodispersed magnetite particles from different organometallic precursors, IEEE Trans. Magn 42 (2006) 3025–3029, 10.1109/TMAG.2006.880111.

[38]. Lee N, Hyeon T, Designed synthesis of uniformly sized iron oxide nanoparticles for efficient magnetic resonance imaging contrast agents, Chem. Soc. Rev 41 (2012) 2575–2589, 10.1039/C1CS15248C. [PubMed: 22138852]

[39]. Park YI, Piao Y, Lee N, Yoo B, Kim BH, Choi SH, Hyeon T, Transformation of hydrophobic iron oxide nanoparticles to hydrophilic and biocompatible maghemite nanocrystals for use as highly efficient MRI contrast agent, J. Mater. Chem21 (2011) 11472–11477, 10.1039/C1JM10432B.

[40]. Thomas LA, Dekker L, Kallumadil M, Southern P, Wilson M, Nair SP, Pankhurst QA, Parkin IP, Carboxylic acid-stabilised iron oxide nanoparticles for use in magnetic hyperthermia, J. Mater. Chem 19 (2009) 6529–6535, 10.1039/B908187A.

[41]. Kotsmar C, Yoon KY, Yu H, Ryoo SY, Barth J, Shao S, Prodanović M, Milner TE, Bryant SL, Huh C, Stable citrate-coated iron oxide superparamagnetic nanoclusters at high salinity, Ind. Eng. Chem. Res 49 (2010) 12435–12443, 10.1021/ie1010965.

[42]. Lee KM, Kim SG, Kim WS, Kim SS, Properties of iron oxide particles prepared in the presence of dextran, Korean J. Chem. Eng 19 (2002) 480–485, 10.1007/BF02697160.

[43]. Liang Y-Y, Zhang L-M, Li W, Chen R-F, Polysaccharide-modified iron oxide nanoparticles as an effective magnetic affinity adsorbent for bovine serum albumin, Colloid Polym. Sci 285 (2007) 1193–1199, 10.1007/s00396-007-1672-2.

[44]. Haviv AH, Grenèche J-M, Lellouche J-P, Aggregation control of hydrophilic maghemite (γ-Fe2O3) nanoparticles by surface doping using cerium atoms, J. Am. Chem. Soc 132 (2010) 12519–12521, 10.1021/ja103283e. [PubMed: 20735060]

[45]. Kluchova K, Zboril R, Tucek J, Pecova M, Zajoncova L, Safarik I, Mashlan M, Markova I, Jancik D, Sebela M, Superparamagnetic maghemite nanoparticles from solid-state synthesis – their functionalization towards peroral MRI contrast agent and magnetic carrier for trypsin immobilization, Biomaterials 30 (2009) 2855–2863, 10.1016/j.biomaterials.2009.02.023. [PubMed: 19264355]

[46]. Jokerst JV, Lobovkina T, Zare RN, Gambhir SS, Nanoparticle PEGylation for imaging and therapy, Nanomedicine 6 (2011) 715–728, 10.2217/nnm.11.19. [PubMed: 21718180]

[47]. Giamblanco N, Marletta G, Graillot A, Bia N, Loubat C, Berret J-F, Serum protein-resistant behavior of multisite-bound poly(ethylene glycol) chains on iron oxide surfaces, ACS Omega 2 (2017) 1309–1320, 10.1021/acsomega.7b00007. [PubMed: 31457506]

[48]. Stepien G, Moros M, Pérez-Hernández M, Monge M, Gutiérrez L, Fratila RM, las Heras M.d., Menao Guillén S, Puente Lanzarote JJ, Solans C, Pardo J, de la Fuente JM, Effect of surface chemistry and associated protein corona on the long-term biodegradation of iron oxide nanoparticles in vivo, ACS Appl. Mater. Interfaces 10 (2018) 4548–4560, 10.1021/acsami.7b18648. [PubMed: 29328627]

[49]. Monopoli MP, Åberg C, Salvati A, Dawson KA, Biomolecular coronas provide the biological identity of nanosized materials, Nat. Nanotechnol 7 (2012) 779–786, 10.1038/nnano.2012.207. [PubMed: 23212421]

[50]. Hurley KR, Lin Y-S, Zhang J, Egger SM, Haynes CL, Effects of mesoporous silica coating and postsynthetic treatment on the transverse relaxivity of iron oxide nanoparticles, Chem. Mater 25 (2013) 1968–1978, 10.1021/cm400711h. [PubMed: 23814377]

[51]. Hurley KR, Ring HL, Etheridge M, Zhang J, Gao Z, Shao Q, Klein ND, Szlag VM, Chung C, Reineke TM, Predictable heating and positive MRI contrast from a mesoporous silica-coated iron oxide nanoparticle, Mol. Pharm 13 (2016) 2172–2183, 10.1021/acs.molpharmaceut.5b00866. [PubMed: 26991550]

[52]. Azhdarzadeh M, Atyabi F, Saei AA, Varnamkhasti BS, Omidi Y, Fateh M, Ghavami M, Shanehsazzadeh S, Dinarvand R, Theranostic MUC-1 aptamer targeted gold coated superparamagnetic iron oxide nanoparticles for magnetic resonance imaging and photothermal therapy of colon cancer, Colloids Surf. B: Biointerfaces 143 (2016) 224–232, 10.1016/j.colsurfb.2016.02.058. [PubMed: 27015647]

[53]. Shirvalilou S, Khoei S, Khoee S, Raoufi NJ, Karimi MR, Shakeri-Zadeh A, Development of a magnetic nano-graphene oxide carrier for improved glioma-targeted drug delivery and imaging: in vitro and in vivo evaluations, Chem. Biol. Interact 295 (2018) 97–108, 10.1016/j.cbi.2018.08.027. [PubMed: 30170108]

[54]. Herd H, Daum N, Jones AT, Huwer H, Ghandehari H, Lehr C-M, Nanoparticle geometry and surface orientation influence mode of cellular uptake, ACS Nano 7 (2013) 1961–1973, 10.1021/nn304439f. [PubMed: 23402533]

[55]. Horák D, Babic M, Jendelová P, Herynek V, Trchová M, Likavcanová K, Kapcalová M, Hájek M, Syková E, Effect of different magnetic nanoparticle coatings on the efficiency of stem cell labeling, J. Magn. Magn. Mater 321 (2009) 1539–1547, 10.1016/j.jmmm.2009.02.082.

[56]. Jana NR, Chen Y, Peng X, Size-and shape-controlled magnetic (Cr, Mn, Fe, Co, Ni) oxide nanocrystals via a simple and general approach, Chem. Mater 16 (2004) 3931–3935, 10.1021/cm049221k.

[57]. Jeon S, Subbiah R, Bonaedy T, Van S, Park K, Yun K, Surface functionalized magnetic nanoparticles shift cell behavior with on/off magnetic fields, J. Cell.Physiol 233 (2018) 1168–1178, 10.1002/jcp.25980. [PubMed: 28464242]

[58]. Jiang S, Eltoukhy AA, Love KT, Anderson DG, Lipidoid-coated iron oxide nanoparticles for efficient DNA and siRNA delivery, Nano Lett. 13 (2013) 1059–1064, 10.1021/nl304287a. [PubMed: 23394319]

[59]. Laurent S, Forge D, Port M, Roch A, Robic C, Vander Elst L, Muller RN, Magnetic iron oxide nanoparticles: synthesis, stabilization, vectorization, physicochemical characterizations, and biological applications, Chem. Rev 108 (2008) 2064–2110, 10.1021/cr068445e. [PubMed: 18543879]

[60]. Shang L, Nienhaus K, Nienhaus GU, Engineered nanoparticles interacting with cells: size matters, J. Nanobiotechnol 12 (2014) 5, 10.1186/14773155-12-5.

[61]. Narkhede AA, Sherwood JA, Antone A, Coogan KR, Bolding MS, Deb S, Bao Y, Rao SS, Role of surface chemistry in mediating the uptake of ultrasmall iron oxide nanoparticles by cancer cells, ACS Appl. Mater. Interfaces 11 (2019) 17157–17166, 10.1021/acsami.9b00606. [PubMed: 31017392]

[62]. Israel LL, Lellouche E, Ostrovsky S, Yarmiayev V, Bechor M, Michaeli S, Lellouche JP, Acute in vivo toxicity mitigation of PEI-coated maghemite nanoparticles using controlled oxidation and surface modifications towards siRNA delivery, ACS Appl. Mater. Interfaces 7 (2015) 15240–15255, 10.1021/acsami.5b0274310.1021/acsami.1025b02743. [PubMed: 26120905]

[63]. Israel LL, Kovalenko EI, Boyko AA, Sapozhnikov AM, Rosenberger I, Kreuter J, Passoni L, Lellouche J-P, Towards hybrid biocompatible magnetic rHuman serum albumin-based nanoparticles: use of ultra-small (CeL n) 3/4+ cation-doped maghemite nanoparticles as functional shell, Nanotechnology 26 (2015) 045601, , 10.1088/0957-4484/26/4/045601.

[64]. Shevtsov MA, Nikolaev BP, Yakovleva LY, Marchenko YY, Dobrodumov AV, Mikhrina AL, Martynova MG, Bystrova OA, Yakovenko IV, Ischenko AM, Superparamagnetic iron oxide nanoparticles conjugated with epidermal growth factor (SPION–EGF) for targeting brain tumors, Int. J. Nanomedicine 9 (2014) 273–287, 10.2147/IJN.S55118. [PubMed: 24421639]

[65]. Lellouche E, Israel LL, Bechor M, Attal S, Kurlander E, Asher VA, Dolitzky A, Shaham L, Izraeli S, Lellouche JP, Michaeli S, MagRET nanoparticles: an iron oxide nanocomposite platform for gene silencing from microRNAs to long non-coding RNAs, Bioconjug. Chem 26 (2015) 1692–1701, 10.1021/acs.bioconjchem.5b00276. [PubMed: 26056709]

[66]. Bullivant JP, Zhao S, Willenberg BJ, Kozissnik B, Batich CD, Dobson J, Materials characterization of feraheme/ferumoxytol and preliminary evaluation of its potential for magnetic fluid hyperthermia, Int. J. Mol. Sci 14 (2013) 17501–17510, 10.3390/ijms140917501. [PubMed: 24065092]

[67]. Zanganeh S, Hutter G, Spitler R, Lenkov O, Mahmoudi M, Shaw A, Pajarinen JS, Nejadnik H, Goodman S, Moseley M, Iron oxide nanoparticles inhibit tumour growth by inducing pro-inflammatory macrophage polarization in tumour tissues, Nat. Nanotechnol 11 (2016) 986–994, 10.1038/nnano.2016.168. [PubMed: 27668795]

[68]. Fütterer S, Andrusenko I, Kolb U, Hofmeister W, Langguth P, Structural characterization of iron oxide/hydroxide nanoparticles in nine different parenteral drugs for the treatment of iron deficiency anaemia by electron diffraction (ED) and X-ray powder diffraction (XRPD), J. Pharm. Biomed. Anal 86 (2013) 151–160, 10.1016/j.jpba.2013.08.005. [PubMed: 23998966]

[69]. Zhang H, Li L, Liu XL, Jiao J, Ng C-T, Yi JB, Luo YE, Bay B-H, Zhao LY, Peng ML, Gu N, Fan HM, Ultrasmall ferrite nanoparticles synthesized via dynamic simultaneous thermal decomposition for high-performance and multifunctional T1 magnetic resonance imaging contrast agent, ACS Nano 11 (2017) 3614–3631, 10.1021/acsnano.6b07684. [PubMed: 28371584]

[70]. Albanese A, Tang PS, Chan WC, The effect of nanoparticle size, shape, and surface chemistry on biological systems, Annu. Rev. Biomed. Eng 14 (2012) 1–16, 10.1146/annurev-bioeng-071811-150124. [PubMed: 22524388]

[71]. Kreuter J, Influence of the surface properties on nanoparticle-mediated transport of drugs to the brain, J. Nanosci. Nanotechnol 4 (2004) 484–488, 10.1166/jnn.2003.077. [PubMed: 15503433]

[72]. Kulkarni SA, Feng S-S, Effects of surface modification on delivery efficiency of biodegradable nanoparticles across the blood–brain barrier, Nanomedicine 6 (2011) 377–394, 10.2217/nnm.10.131. [PubMed: 21385139]

[73]. Verma A, Stellacci F, Effect of surface properties on nanoparticle–cell interactions, Small 6 (2010) 12–21, 10.1002/smll.200901158. [PubMed: 19844908]

[74]. Arvizo RR, Miranda OR, Thompson MA, Pabelick CM, Bhattacharya R, Robertson JD, Rotello VM, Prakash Y, Mukherjee P, Effect of nanoparticle surface charge at the plasma membrane and beyond, Nano Lett. 10 (2010) 2543–2548, 10.1021/nl101140t. [PubMed: 20533851]

[75]. Zhang Y, Yang M, Portney NG, Cui D, Budak G, Ozbay E, Ozkan M, Ozkan CS, Zeta potential: a surface electrical characteristic to probe the interaction of nanoparticles with normal and cancer human breast epithelial cells, Biomed. Microdevices 10 (2008) 321–328, 10.1007/s10544-007-9139-2. [PubMed: 18165903]

[76]. Blanchette M, Daneman R, Formation and maintenance of the BBB, Mech. Dev 138 (2015) 8–16, 10.1016/j.mod.2015.07.007. [PubMed: 26215350]

[77]. Zhao Z, Nelson AR, Betsholtz C, Zlokovic BV, Establishment and dysfunction of the blood-brain barrier, Cell 163 (2015) 1064–1078, 10.1016/j.cell.2015.10.067. [PubMed: 26590417]

[78]. Pardridge WM, Blood-brain barrier endogenous transporters as therapeutic targets: a new model for small molecule CNS drug discovery, Expert Opin. Ther.Targets 19 (2015) 1059–1072, 10.1517/14728222.2015.1042364. [PubMed: 25936389]

[79]. Ljubimova JY, Sun T, Mashouf L, Ljubimov AV, Israel LL, Ljubimov VA, Falahatian V, Holler E, Covalent nano delivery systems for selective imaging and treatment of brain tumors, Adv. Drug Deliv. Rev 113 (2017) 177–200, 10.1016/j.addr.2017.06.002. [PubMed: 28606739]

[80]. Lockman PR, Mittapalli RK, Taskar KS, Rudraraju V, Gril B, Bohn KA, Adkins CE, Roberts A, Thorsheim HR, Gaasch JA, Heterogeneous blood–tumor barrier permeability determines drug efficacy in experimental brain metastases of breast cancer, Clin. Cancer Res 16 (2010) 5664–5678, 10.1158/1078-0432.CCR-10-1564. [PubMed: 20829328]

[81]. Khaitan D, Reddy PL, Narayana DS, Ningaraj NS, Chapter 17 – Recent advances in understanding of blood–brain tumor barrier (BTB) permeability mechanisms that enable better detection and treatment of brain tumors, in:Grumezescu AM (Ed.), Drug Targeting and Stimuli Sensitive Drug Delivery Systems, William Andrew Publishing, 2018, pp. 673–688.

[82]. Carmeliet P, Jain RK, Principles and mechanisms of vessel normalization for cancer and other angiogenic diseases, Nat. Rev. Drug Discov 10 (2011) 417–427, 10.1038/nrd3455. [PubMed: 21629292]

[83]. Anchordoquy TJ, Barenholz Y, Boraschi D, Chorny M, Decuzzi P, Dobrovolskaia MA, Farhangrazi ZS, Farrell D, Gabizon A, Ghandehari H, Godin B, La-Beck NM, Ljubimova J, Moghimi SM, Pagliaro L, Park J-H, Peer D, Ruoslahti E, Serkova NJ, Simberg D, Mechanisms and barriers in cancer nanomedicine: addressing challenges, looking for solutions, ACS Nano 11 (2017) 12–18, 10.1021/acsnano.6b08244. [PubMed: 28068099]

[84]. Danhier F, To exploit the tumor microenvironment: since the EPR effect fails in the clinic, what is the future of nanomedicine? J. Control. Release 244 (2016) 108–121, 10.1016/j.jconrel.2016.11.015. [PubMed: 27871992]

[85]. Ruan S, Qin L, Xiao W, Hu C, Zhou Y, Wang R, Sun X, Yu W, He Q, Gao H, Acid-responsive transferrin dissociation and GLUT mediated exocytosis for increased blood–brain barrier transcytosis and programmed glioma targeting delivery, Adv. Funct. Mater 28 (2018) 1802227, , 10.1002/adfm.201802227.

[86]. Inoue S, Patil R, Portilla-Arias J, Ding H, Konda B, Espinoza A, Mongayt D, Markman JL, Elramsisy A, Phillips HW, Black KL, Holler E, Ljubimova JY, Nanobiopolymer for direct targeting and inhibition of EGFR expression in triple negative breast cancer, PLoS One 7 (2012) e31070, , 10.1371/journal.pone.0031070.

[87]. The Human Protein Atlas. version 19.1, https://www.proteinatlas.org.

[88]. Ren J, Shen S, Wang D, Xi Z, Guo L, Pang Z, Qian Y, Sun X, Jiang X, The targeted delivery of anticancer drugs to brain glioma by PEGylated oxidized multi-walled carbon nanotubes modified with angiopep-2, Biomaterials 33 (2012) 3324–3333, 10.1016/j.biomaterials.2012.01.025. [PubMed: 22281423]

[89]. de Paula Aguiar MF, Mamani JB, Felix TK, dos Reis RF, da Silva HR, Nucci LP, Nucci-da-Silva MP, Gamarra LF, Magnetic targeting with superparamagnetic iron oxide nanoparticles for in vivo glioma, Nanotechnol. Rev 6 (2017) 449–472, 10.1515/ntrev-2016-0101.

[90]. Qiu Y, Tong S, Zhang L, Sakurai Y, Myers DR, Hong L, Lam WA, Bao G, Magnetic forces enable controlled drug delivery by disrupting endothelial cell-cell junctions, Nat. Commun 8 (2017) 15594, , 10.1038/ncomms15594. [PubMed: 28593939]

[91]. von der Ecken J, Müller M, Lehman W, Manstein DJ, Penczek PA, Raunser S, Structure of the F-actin–tropomyosin complex, Nature 519 (2014) 114–117, 10.1038/nature14033. [PubMed: 25470062]

[92]. Kong SD, Lee J, Ramachandran S, Eliceiri BP, Shubayev VI, Lal R, Jin S, Magnetic targeting of nanoparticles across the intact blood–brain barrier, J. Control. Release 164 (2012) 49–57, 10.1016/j.jconrel.2012.09.021. [PubMed: 23063548]

[93]. Chertok B, David AE, Yang VC, Polyethyleneimine-modified iron oxide nanoparticles for brain tumor drug delivery using magnetic targeting and intra-carotid administration, Biomaterials 31 (2010) 6317–6324, 10.1016/j.biomaterials.2010.04.043. [PubMed: 20494439]

[94]. Huang Y, Zhang B, Xie S, Yang B, Xu Q, Tan J, Superparamagnetic iron oxide nanoparticles modified with Tween 80 pass through the intact blood–brain barrier in rats under magnetic field, ACS Appl. Mater. Interfaces 8 (2016) 11336–11341, 10.1021/acsami.6b02838. [PubMed: 27092793]

[95]. Vinzant N, Scholl JL, Wu C-M, Kindle T, Koodali R, Forster GL, Iron oxide nanoparticle delivery of peptides to the brain: reversal of anxiety during drug withdrawal, Front. Neurosci 11 (2017) 608, 10.3389/fnins.2017.00608. [PubMed: 29163012]

[96]. Busquets MA, Espargaró A, Sabaté R, Estelrich J, Magnetic nanoparticles cross the blood-brain barrier: when physics rises to a challenge, Nanomaterials 5 (2015) 2231–2248, 10.3390/nano5042231. [PubMed: 28347118]

[97]. Dan M, Bae Y, Pittman TA, Yokel RA, Alternating magnetic field-induced hyperthermia increases iron oxide nanoparticle cell association/uptake and flux in blood–brain barrier models, Pharm. Res 32 (2015) 1615–1625, 10.1007/s11095-014-1561-6. [PubMed: 25377069]

[98]. Tabatabaei SN, Girouard H, Carret A-S, Martel S, Remote control of the permeability of the blood–brain barrier by magnetic heating of nanoparticles: a proof of concept for brain drug delivery, J. Control. Release 206 (2015) 49–57, 10.1016/j.jconrel.2015.02.027. [PubMed: 25724273]

[99]. Lammers T, Koczera P, Fokong S, Gremse F, Ehling J, Vogt M, Pich A, Storm G, Van Zandvoort M, Kiessling F, Theranostic USPIO-loaded microbubbles for mediating and monitoring blood-brain barrier permeation, Adv. Funct. Mater25 (2015) 36–43, 10.1002/adfm.201401199. [PubMed: 25729344]

[100]. Sun Z, Worden M, Thliveris JA, Hombach-Klonisch S, Klonisch T, van Lierop J, Hegmann T, Miller DW, Biodistribution of negatively charged iron oxide nanoparticles (IONPs) in mice and enhanced brain delivery using lysophosphatidic acid (LPA), Nanomedicine 12 (2016) 1775–1784, 10.1016/j.nano.2016.04.008. [PubMed: 27125435]

[101]. Neuwelt EA, Varallyay P, Bago A, Muldoon L, Nesbit G, Nixon R, Imaging of iron oxide nanoparticles by MR and light microscopy in patients with malignant brain tumours, Neuropathol. Appl. Neurobiol 30 (2004) 456–471, 10.1111/j.1365-2990.2004.00557.x. [PubMed: 15488022]

[102]. Chertok B, Moffat BA, David AE, Yu F, Bergemann C, Ross BD, Yang VC, Iron oxide nanoparticles as a drug delivery vehicle for MRI monitored magnetic targeting of brain tumors, Biomaterials 29 (2008) 487–496, 10.1016/j.biomaterials.2007.08.050. [PubMed: 17964647]

[103]. Kircher MF, De La Zerda A, Jokerst JV, Zavaleta CL, Kempen PJ, Mittra E, Pitter K, Huang R, Campos C, Habte F, A brain tumor molecular imaging strategy using a new triple-modality MRI-photoacoustic-raman nanoparticle, Nat. Med 18 (2012) 829–834, 10.1038/nm.2721. [PubMed: 22504484]

[104]. Maeda H, Wu J, Sawa T, Matsumura Y, Hori K, Tumor vascular permeability and the EPR effect in macromolecular therapeutics: a review, J. Control. Release 65 (2000) 271–284, 10.1016/S0168-3659(99)00248-5. [PubMed: 10699287]

[105]. Richard S, Saric A, Boucher M, Slomianny C, Geffroy F, Mériaux S, Lalatonne Y, Petit PX, Motte L, Antioxidative theranostic iron oxide nanoparticles toward brain tumors imaging and ROS production, ACS Chem. Biol 11 (2016) 2812–2819, 10.1021/acschembio.6b00558. [PubMed: 27513597]

[106]. Sun L, Joh DY, Al-Zaki A, Stangl M, Murty S, Davis JJ, Baumann BC, Alonso-Basanta M, Kao GD, Tsourkas A, Theranostic application of mixed gold and superparamagnetic iron oxide nanoparticle micelles in glioblastoma multiforme, J. Biomed. Nanotechnol 12 (2016) 347–356, 10.1166/jbn.2016.2173. [PubMed: 27305768]

[107]. Srimanee A, Regberg J, Hallbrink M, Kurrikoff K, Veiman K-L, Vajragupta O, Langel Ü, Peptide-based delivery of oligonucleotides across blood–brain barrier model, Int. J. Pept. Res. Ther 20 (2014) 169–178, 10.1007/s10989-013-9378-4.

[108]. Patil R, Ljubimov AV, Gangalum PR, Ding H, Portilla-Arias J, Wagner S, Inoue S, Konda B, Rekechenetskiy A, Chesnokova A, Markman JL, Ljubimov VA, Li D, Prasad RS, Black KL, Holler E, Ljubimova JY, MRI virtual biopsy and treatment of brain metastatic tumors with targeted nanobioconjugates: nanoclinic in the brain, ACS Nano 9 (2015) 5594–5608, 10.1021/acsnano.5b01872. [PubMed: 25906400]

[109]. Kou L, Hou Y, Yao Q, Guo W, Wang G, Wang M, Fu Q, He Z, Ganapathy V, Sun J, L-Carnitine-conjugated nanoparticles to promote permeation across blood–brain barrier and to target glioma cells for drug delivery via the novel organic cation/carnitine transporter OCTN2, Artif. Cells Nanomed. Biotechnol 46 (2018) 1605–1616 1–12 10.1080/21691401.2017.1384385. [PubMed: 28974108]

[110]. Lajoie JM, Shusta EV, Targeting receptor-mediated transport for delivery of biologics across the blood-brain barrier, Annu. Rev. Pharmacol. Toxicol 55 (2015) 613–631, 10.1146/annurev-pharmtox-010814-124852. [PubMed: 25340933]

[111]. Dautry-Varsat A, Ciechanover A, Lodish HF, pH and the recycling of transferrin during receptor-mediated endocytosis, Proc. Natl. Acad. Sci 80 (1983) 2258–2262, 10.1073/pnas.80.8.2258. [PubMed: 6300903]

[112]. Saraiva C, Praça C, Ferreira R, Santos T, Ferreira L, Bernardino L, Nanoparticle-mediated brain drug delivery: overcoming blood–brain barrier to treat neurodegenerative diseases, J. Control. Release 235 (2016) 34–47, 10.1016/j.jconrel.2016.05.044. [PubMed: 27208862]

[113]. Jefferies WA, Brandon MR, Hunt SV, Williams AF, Gatter KC, Mason DY, Transferrin receptor on endothelium of brain capillaries, Nature 312 (1984) 162. [PubMed: 6095085]

[114]. Ghadiri M, Vasheghani-Farahani E, Atyabi F, Kobarfard F, Mohamadyar-Toupkanlou F, Hosseinkhani H, Transferrin-conjugated magnetic dextran-spermine nanoparticles for targeted drug transport across blood-brain barrier, J. Biomed. Mater. Res. A 105 (2017) 2851–2864, 10.1002/jbm.a.36145. [PubMed: 28639394]

[115]. Tian X, Nyberg S, Madsen SP,J, Daneshpour N, Armes SP, Berwick J, Azzouz M, Shaw P, Abbott NJ, Battaglia G, LRP-1-mediated intracellular antibody delivery to the central nervous system, Sci. Rep 5 (2015), 10.1038/srep1199011990.

[116]. Bell RD, Sagare AP, Friedman AE, Bedi GS, Holtzman DM, Deane R, Zlokovic BV, Transport pathways for clearance of human Alzheimer's amyloid β-peptide and apolipoproteins E and J in the mouse central nervous system, J. Cereb. Blood Flow Metab 27 (2007) 909–918, 10.1038/sj.jcbfm.9600419. [PubMed: 17077814]

[117]. Demeule M, Currie JC, Bertrand Y, Che C, Nguyen T, Regina A, Gabathuler R, Castaigne JP, Beliveau R, Involvement of the low-density lipoprotein receptor-related protein in the transcytosis of the brain delivery vector Angiopep-2, J. Neurochem 106 (2008) 1534–1544, 10.1111/j.1471-4159.2008.05492.x. [PubMed: 18489712]

[118]. Chen G-J, Su Y-Z, Hsu C, Lo Y-L, Huang S-J, Ke J-H, Kuo Y-C, Wang L-F, Angiopep-pluronic F127-conjugated superparamagnetic iron oxide nanoparticles as nanotheranostic agents for BBB targeting, J. Mater. Chem. B 2 (2014) 5666–5675, 10.1039/C4TB00543K. [PubMed: 32262201]

[119]. Israel LL, Braubach O, Galstyan A, Chiechi A, Shatalova ES, Grodzinski Z, Ding H, Black KL, Ljubimova JY, Holler E, A combination of tri-leucine and angiopep-2 drives a poly-anionic polymalic acid nanodrug platform across the blood-brain barrier, ACS Nano 13 (2019) 1253–1271, 10.1021/acsnano.8b06437. [PubMed: 30633492]

[120]. Boado RJ, Lu JZ, Hui EK-W, Lin H, Pardridge WM, Insulin receptor antibody−α-N-acetylglucosaminidase fusion protein penetrates the primate blood–brain barrier and reduces glycosoaminoglycans in Sanfilippo Type B fibroblasts, Mol. Pharm 13 (2016) 1385–1392, 10.1021/acs.molpharmaceut.6b00037. [PubMed: 26910785]

[121]. Jiang X, Sha X, Xin H, Xu X, Gu J, Xia W, Chen S, Xie Y, Chen L, Chen Y, Integrin-facilitated transcytosis for enhanced penetration of advanced gliomas by poly (trimethylene carbonate)-based nanoparticles encapsulating paclitaxel, Biomaterials 34 (2013) 2969–2979, 10.1016/j.biomaterials.2012.12.049. [PubMed: 23380351]

[122]. Bellis SL, Advantages of RGD peptides for directing cell association with biomaterials, Biomaterials 32 (2011) 4205–4210, 10.1016/j.biomaterials.2011.02.029. [PubMed: 21515168]

[123]. Oller-Salvia B, Sánchez-Navarro M, Giralt E, Teixidó M, Blood–brain barrier shuttle peptides: an emerging paradigm for brain delivery, Chem. Soc. Rev 45 (2016) 4690–4707, 10.1039/C6CS00076B. [PubMed: 27188322]

[124]. Gao H, Xiong Y, Zhang S, Yang Z, Cao S, Jiang X, RGD and interleukin-13 peptide functionalized nanoparticles for enhanced glioblastoma cells and neo-vasculature dual targeting delivery and elevated tumor penetration, Mol. Pharm 11 (2014) 1042–1052, 10.1021/mp400751g. [PubMed: 24521297]

[125]. Melemenidis S, Jefferson A, Ruparelia N, Akhtar AM, Xie J, Allen D, Hamilton A, Larkin JR, Perez-Balderas F, Smart SC, Molecular magnetic resonance imaging of angiogenesis in vivo using polyvalent cyclic RGD-iron oxide microparticle conjugates, Theranostics 5 (2015) 515–529, 10.7150/thno.10319. [PubMed: 25767618]

[126]. Yang J, Luo Y, Xu Y, Li J, Zhang Z, Wang H, Shen M, Shi X, Zhang G, Conjugation of iron oxide nanoparticles with RGD-modified dendrimers for targeted tumor MR imaging, ACS Appl. Mater. Interfaces 7 (2015) 5420–5428, 10.1021/am508983n. [PubMed: 25695661]

[127]. Boucher M, Geffroy F, Prévéral S, Bellanger L, Selingue E, Adryanczyk-Perrier G, Péan M, Lefèvre C, Pignol D, Ginet N, Genetically tailored magnetosomes used as MRI probe for molecular imaging of brain tumor, Biomaterials 121 (2017) 167–178, 10.1016/j.biomaterials.2016.12.013. [PubMed: 28088078]

[128]. Wang Y-XJ, Superparamagnetic iron oxide based MRI contrast agents: current status of clinical application, Quant. Imaging Med. Surg 1 (2011) 35–40, 10.3978/j.issn.2223-4292.2011.08.03. [PubMed: 23256052]

[129]. Israel LL, Karimi F, Bianchessi S, Scanziani E, Passoni L, Matteoli M, Langström B, Lellouche J-P, Surface metal cation doping of maghemite nanoparticles: modulation of MRI relaxivity features and chelator-free 68Ga-radiolabelling for dual MRI-PET imaging, Mater. Res. Exp 2 (2015) 095009, , 10.1088/2053-1591/2/9/095009.

[130]. Ben Ishay R, Israel LL, Levy E, Partouche DM, Lellouche J-P, Maghemite-human serum albumin hybrid nanoparticles: towards a theranostic system with high MRI r2* relaxivity, J. Mater. Chem. B 4 (2016) 3801–3814, 10.1039/C6TB00778C. [PubMed: 32263318]

[131]. Vuong QL, Berret JF, Fresnais J, Gossuin Y, Sandre O, A universal scaling law to predict the efficiency of magnetic nanoparticles as MRI T2-contrast agents, Adv. Healthc. Mater 1 (2012) 502–512, 10.1002/adhm.201200078. [PubMed: 23184784]

[132]. Esquinazi P, Hergert W, Spemann D, Setzer A, Ernst A, Defect-induced magnetism in solids, IEEE Trans. Magn 49 (2013) 4668–4674, 10.1109/TMAG.2013.2255867.

[133]. Andriotis AN, Menon M, The synergistic character of the defect-induced magnetism in diluted magnetic semiconductors and related magnetic materials, J. Phys. Condens. Matter 24 (2012) 455801, , 10.1088/0953-8984/24/45/455801.

[134]. Andriotis AN, Menon M, Defect-induced magnetism: codoping and a prescription for enhanced magnetism, Phys. Rev. B 87 (2013) 155309, , 10.1103/PhysRevB.87.155309.

[135]. Hu Y, Li J, Yang J, Wei P, Luo Y, Ding L, Sun W, Zhang G, Shi X, Shen M, Facile synthesis of RGD peptide-modified iron oxide nanoparticles with ultrahigh relaxivity for targeted MR imaging of tumors, Biomater. Sci 3 (2015) 721–732, 10.1039/C5BM00037H. [PubMed: 26222591]

[136]. Liu Q, Song L, Chen S, Gao J, Zhao P, Du J, A superparamagnetic polymersome with extremely high T2 relaxivity for MRI and cancer-targeted drug delivery, Biomaterials 114 (2017) 23–33, 10.1016/j.biomaterials.2016.10.027. [PubMed: 27837682]

[137]. Wang Y, Xu C, Chang Y, Zhao L, Zhang K, Zhao Y, Gao F, Gao X, Ultrasmall superparamagnetic iron oxide nanoparticle for T2-weighted magnetic resonance imaging, ACS Appl. Mater. Interfaces 9 (2017) 28959–28966, 10.1021/acsami.7b10030. [PubMed: 28786283]

[138]. Xiao W, Legros P, Chevallier P, Lagueux J, Oh JK, Fortin M-A, Superparamagnetic iron oxide nanoparticles stabilized with multidentate block copolymers for optimal vascular contrast in T1-weighted magnetic resonance imagingMRI, ACS Appl. Nano Mater 1 (2018) 894–907, 10.1021/acsanm.7b00300.

[139]. Groult H, Poupard N, Herranz F, Conforto E, Bridiau N, Sannier F, Bordenave S, Piot J-M, Ruiz-Cabello J, Fruitier-Arnaudin I, Maugard T, Family of bioactive heparin-coated iron oxide nanoparticles with positive contrast in magnetic resonance imaging for specific biomedical applications, Biomacromolecules 18 (2017) 3156–3167, 10.1021/acs.biomac.7b00797. [PubMed: 28850787]

[140]. Magnitsky S, Zhang J, Idiyatullin D, Mohan G, Garwood M, Lane NE, Majumdar S, Positive contrast from cells labeled with iron oxide nanoparticles: quantitation of imaging data, Magn. Reson. Med 78 (2017) 1900–1910, 10.1002/mrm.26585. [PubMed: 28097749]

[141]. Zhang J, Ring HL, Hurley KR, Shao Q, Carlson CS, Idiyatullin D, Manuchehrabadi N, Hoopes PJ, Haynes CL, Bischof JC, Garwood M, Quantification and biodistribution of iron oxide nanoparticles in the primary clearance organs of mice using T1 contrast for heating, Magn. Reson. Med 78 (2017) 702–712, 10.1002/mrm.26394. [PubMed: 27667655]

[142]. Pellico J, Ruiz-Cabello J, Fernández-Barahona I, Gutiérrez L, Lechuga-Vieco AV, Enríquez JA, Morales MP, Herranz F, One-step fast synthesis of nanoparticles for MRI: coating chemistry as the key variable determining positive or negative contrast, Langmuir 33 (2017) 10239–10247, 10.1021/acs.langmuir.7b01759. [PubMed: 28882034]

[143]. Wei H, Bruns OT, Kaul MG, Hansen EC, Barch M, Wiśniowska A, Chen O, Chen Y, Li N, Okada S, Exceedingly small iron oxide nanoparticles as positive MRI contrast agents, Proc. Natl. Acad. Sci 114 (2017) 2325–2330 201620145 10.1073/pnas.1620145114. [PubMed: 28193901]

[144]. Wang L, Huang J, Chen H, Wu H, Xu Y, Li Y, Yi H, Wang YA, Yang L, Mao H, Exerting enhanced permeability and retention effect driven delivery by ultrafine iron oxide nanoparticles with T1–T2 switchable magnetic resonance imaging contrast, ACS Nano 11 (2017) 4582–4592, 10.1021/acsnano.7b00038. [PubMed: 28426929]

[145]. Ferguson RM, Khandhar AP, Kemp SJ, Arami H, Saritas EU, Croft LR, Konkle J, Goodwill PW, Halkola A, Rahmer J, Magnetic particle imaging with tailored iron oxide nanoparticle tracers, IEEE Trans. Med. Imaging 34 (2015) 1077–1084, 10.1109/TMI.2014.2375065. [PubMed: 25438306]

[146]. Gleich B, Weizenecker J, Tomographic imaging using the nonlinear response of magnetic particles, Nature 435 (2005) 1214–1217, 10.1038/nature03808. [PubMed: 15988521]

[147]. Knopp T, Gdaniec N, Möddel M, Magnetic particle imaging: from proof of principle to preclinical applications, Phys. Med. Biol 62 (2017) R124, 10.1088/1361-6560/aa6c99.

[148]. Khandhar A, Keselman P, Kemp S, Ferguson R, Goodwill P, Conolly S, Krishnan K, Evaluation of PEG-coated iron oxide nanoparticles as blood pool tracers for preclinical magnetic particle imaging, Nanoscale 9 (2017) 1299–1306, 10.1039/C6NR08468K. [PubMed: 28059427]

[149]. Bulte JW, Walczak P, Janowski M, Krishnan KM, Arami H, Halkola A, Gleich B, Rahmer J, Quantitative “hot spot” imaging of transplanted stem cells using superparamagnetic tracers and magnetic particle imaging (MPI), Tomogr. J. Imaging Res 1 (2015) 91–97, 10.18383/j.tom.2015.00172.

[150]. Sedlacik J, Frölich A, Spallek J, Forkert ND, Faizy TD, Werner F, Knopp T, Krause D, Fiehler J, Buhk J-H, Magnetic particle imaging for high temporal resolution assessment of aneurysm hemodynamics, PLoS One 11 (2016) e0160097, , 10.1371/journal.pone.0160097.

[151]. Zheng B, Marc P, Yu E, Gunel B, Lu K, Vazin T, Schaffer DV, Goodwill PW, Conolly SM, Quantitative magnetic particle imaging monitors the transplantation, biodistribution, and clearance of stem cells in vivo, Theranostics 6 (2016) 291–301, 10.7150/thno.13728. [PubMed: 26909106]

[152]. Zheng B, Vazin T, Goodwill PW, Conway A, Verma A, Saritas EU, Schaffer D, Conolly SM, Magnetic particle imaging tracks the long-term fate of in vivo neural cell implants with high image contrast, Sci. Rep 5 (2015) 14055, , 10.1038/srep14055. [PubMed: 26358296]

[153]. Li X, Zhang X-N, Li X-D, Chang J, Multimodality imaging in nanomedicine and nanotheranostics, Cancer Biol. Med 13 (2016) 339–348, 10.20892/j.issn.2095-3941.2016.0055. [PubMed: 27807501]

[154]. Kim J, Piao Y, Hyeon T, Multifunctional nanostructured materials for multimodal imaging, and simultaneous imaging and therapy, Chem. Soc. Rev 38 (2009) 372–390, 10.1039/B709883A. [PubMed: 19169455]

[155]. Arami H, Khandhar AP, Tomitaka A, Yu E, Goodwill PW, Conolly SM, Krishnan KM, In vivo multimodal magnetic particle imaging (MPI) with tailored magneto/optical contrast agents, Biomaterials 52 (2015) 251–261, 10.1016/j.biomaterials.2015.02.040. [PubMed: 25818431]

[156]. Song X, Gong H, Yin S, Cheng L, Wang C, Li Z, Li Y, Wang X, Liu G, Liu Z, Ultra-small iron oxide doped polypyrrole nanoparticles for in vivo multimodal imaging guided photothermal therapy, Adv. Funct. Mater 24 (2014) 1194–1201, 10.1002/adfm.201302463.

[157]. Hwang DW, Ko HY, Kim SK, Kim D, Lee DS, Kim S, Development of a quadruple imaging modality by using nanoparticles, Chem. Eur. J 15 (2009) 9387–9393, 10.1002/chem.200900344. [PubMed: 19658128]

[158]. Locatelli E, Gil L, Israel LL, Passoni L, Naddaka M, Pucci A, Reese T, Gomez-Vallejo V, Milani P, Matteoli M, Biocompatible nanocomposite for PET/MRI hybrid imaging, Int. J. Nanomedicine 7 (2012) 6021–6033, 10.2147/IJN.S38107. [PubMed: 23271907]

[159]. Reguera J, de Aberasturi DJ, Henriksen-Lacey M, Langer J, Espinosa A, Szczupak B, Wilhelm C, Liz-Marzán LM, Janus plasmonic–magnetic gold–iron oxide nanoparticles as contrast agents for multimodal imaging, Nanoscale 9 (2017) 9467–9480, 10.1039/C7NR01406F. [PubMed: 28660946]

[160]. Xie J, Chen K, Huang J, Lee S, Wang J, Gao J, Li X, Chen X, PET/NIRF/MRI triple functional iron oxide nanoparticles, Biomaterials 31 (2010) 3016–3022, 10.1016/j.biomaterials.2010.01.010. [PubMed: 20092887]

[161]. Wu Y, Gao D, Zhang P, Li C, Wan Q, Chen C, Gong P, Gao G, Sheng Z, Cai L, Iron oxide nanoparticles protected by NIR-active multidentate-polymers as multifunctional nanoprobes for NIRF/PA/MR trimodal imaging, Nanoscale 8 (2016) 775–779, 10.1039/C5NR06660C. [PubMed: 26658484]

[162]. Xia J, Yao J, Wang LV, Photoacoustic tomography: principles and advances, Electromagn. Waves (Cambridge, Mass.) 147 (2014) 1–22, 10.2528/pier14032303.

[163]. Pahari SK, Olszakier S, Kahn I, Amirav L, Magneto-fluorescent yolk–shell nanoparticles, Chem. Mater 30 (2018) 775–780, 10.1021/acs.chemmater.7b04253.

[164]. Liu T, Shi S, Liang C, Shen S, Cheng L, Wang C, Song X, Goel S, Barnhart TE, Cai W, Iron oxide decorated MoS2 nanosheets with double PEGylation for chelator-free radiolabeling and multimodal imaging guided photothermal therapy, ACS Nano 9 (2015) 950–960, 10.1021/nn506757x. [PubMed: 25562533]

[165]. Nemati Z, Alonso J, Rodrigo I, Das R, Garaio E, García JÁ, Orue I, Phan M-H, Srikanth H, Improving the heating efficiency of iron oxide nanoparticles by tuning their shape and size, J. Phys. Chem. C 122 (2018) 2367–2381, 10.1021/acs.jpcc.7b10528.

[166]. Niculaes D, Lak A, Anyfantis GC, Marras S, Laslett O, Avugadda SK, Cassani M, Serantes D, Hovorka O, Chantrell R, Pellegrino T, Asymmetric assembling of iron oxide nanocubes for improving magnetic hyperthermia performance, ACS Nano 11 (2017) 12121–12133, 10.1021/acsnano.7b05182. [PubMed: 29155560]

[167]. Mazuel F, Espinosa A, Radtke G, Bugnet M, Neveu S, Lalatonne Y, Botton GA, Abou-Hassan A, Wilhelm C, Magneto-thermal metrics can mirror the long-term intracellular fate of magneto-plasmonic nanohybrids and reveal the remarkable shielding effect of gold, Adv. Funct. Mater 27 (2017), 10.1002/adfm.2016059971605997-n/a.

[168]. Laurent S, Dutz S, Häfeli UO, Mahmoudi M, Magnetic fluid hyperthermia: focus on superparamagnetic iron oxide nanoparticles, Adv. Colloid Interf. Sci 166 (2011) 8–23, 10.1016/j.cis.2011.04.003.

[169]. Bauer LM, Situ SF, Griswold MA, Samia ACS, High-performance iron oxide nanoparticles for magnetic particle imaging–guided hyperthermia (hMPI), Nanoscale 8 (2016) 12162–12169, 10.1039/C6NR01877G. [PubMed: 27210742]

[170]. Espinosa A, Di Corato R, Kolosnjaj-Tabi J, Flaud P, Pellegrino T, Wilhelm C, Duality of iron oxide nanoparticles in cancer therapy: amplification of heating efficiency by magnetic hyperthermia and photothermal bimodal treatment, ACS Nano 10 (2016) 2436–2446, 10.1021/acsnano.5b07249. [PubMed: 26766814]

[171]. Kang H, Kim S, Wong DSH, Jung HJ, Lin S, Zou K, Li R, Li G, Dravid VP, Bian L, Remote manipulation of ligand nano-oscillations regulates adhesion and polarization of macrophages in vivo, Nano Lett. 17 (2017) 6415–6427, 10.1021/acs.nanolett.7b03405. [PubMed: 28875707]

[172]. Tong H-I, Kang W, Shi Y, Zhou G, Lu Y, Physiological function and inflamed-brain migration of mouse monocyte-derived macrophages following cellular uptake of superparamagnetic iron oxide nanoparticles—implication of macrophage-based drug delivery into the central nervous system, Int. J. Pharm 505 (2016) 271–282, 10.1016/j.ijpharm.2016.03.028. [PubMed: 27001531]

[173]. Harrison R, Markides H, Morris RH, Richards P, El Haj AJ, Sottile V, Autonomous magnetic labelling of functional mesenchymal stem cells for improved traceability and spatial control in cell therapy applications, J. Tissue Eng.Regen. Med 11 (2017) 2333–2348, 10.1002/term.2133. [PubMed: 27151571]

[174]. Yang Q, Joy G, Christopher JM, Feng G, Richard B, Frederick FL, Stafford RJ, Marites PM, Magnetic resonance and photoacoustic imaging of brain tumor mediated by mesenchymal stem cell labeled with multifunctional nanoparticle introduced via carotid artery injection, Nanotechnology 29 (2018) 165101, , 10.1088/1361-6528/aaaf16.

[175]. Adams C, Israel LL, Ostrovsky S, Taylor A, Poptani H, Lellouche J-P, Chari D, Development of multifunctional magnetic nanoparticles for genetic engineering and tracking of neural stem cells, Advan. Healthc. Mater 5 (2016) 841–849, 10.1002/adhm.201500885. [PubMed: 26867130]

[176]. Inoue S, Ding H, Portilla-Arias J, Hu J, Konda B, Fujita M, Espinoza A, Suhane S, Riley M, Gates M, Polymalic acid–based nanobiopolymer provides efficient systemic breast cancer treatment by inhibiting both HER2/neu receptor synthesis and activity, Cancer Res. 71 (2011) 1454–1464, 10.1158/0008-5472.CAN-10-3093. [PubMed: 21303974]

[177]. Ljubimova JY, Portilla-Arias J, Patil R, Ding H, Inoue S, Markman JL, Rekechenetskiy A, Konda B, Gangalum PR, Chesnokova A, Ljubimov AV, Black KL, Holler E, Toxicity and efficacy evaluation of multiple targeted polymalic acid conjugates for triple-negative breast cancer treatment, J. Drug Target 21 (2013) 956–967, 10.3109/1061186X.2013.837470. [PubMed: 24032759]

[178]. Ljubimova JY, Fujita M, Ljubimov AV, Torchilin VP, Black KL, Holler E, Poly (malic acid) nanoconjugates containing various antibodies and oligonucleotides for multitargeting drug delivery, Nanomedicine 3 (2008) 247–265, 10.2217/17435889.3.2.247. [PubMed: 18373429]

[179]. Ljubimova JY, Ding H, Portilla-Arias J, Patil R, Gangalum PR, Chesnokova A, Inoue S, Rekechenetskiy A, Nassoura T, Black KL, Polymalic acid-based nano biopolymers for targeting of multiple tumor markers: an opportunity for personalized medicine? J. Vis. Exp 88 (2014), 10.3791/50668e50668.

[180]. Timbie KF, Mead BP, Price RJ, Drug and gene delivery across the blood–brain barrier with focused ultrasound, J. Control. Release 219 (2015) 61–75, 10.1016/j.jconrel.2015.08.059. [PubMed: 26362698]

[181]. Sachdeva M, Sachdeva N, Pal M, Gupta N, Khan IA, Majumdar M, Tiwari A, CRISPR/Cas9: molecular tool for gene therapy to target genome and epigenome in the treatment of lung cancer, Cancer Gene Ther. 22 (2015) 509–517, 10.1038/cgt.2015.54. [PubMed: 26494554]

[182]. Novo L, Takeda KM, Petteta T, Dakwar GR, van den Dikkenberg JB, Remaut K, Braeckmans K, van Nostrum CF, Mastrobattista E, Hennink WE, Targeted decationized polyplexes for siRNA delivery, Mol. Pharm 12 (2015) 150–161, 10.1021/mp500499x. [PubMed: 25384057]

[183]. Lo Y-L, Chou H-L, Liao Z-X, Huang S-J, Ke J-H, Liu Y-S, Chiu C-C, Wang L-F, Chondroitin sulfate-polyethylenimine copolymer-coated superparamagnetic iron oxide nanoparticles as an efficient magneto-gene carrier for microRNA-encoding plasmid DNA delivery, Nanoscale 7 (2015) 8554–8565, 10.1039/C5NR01404B. [PubMed: 25897645]

[184]. Xiao S, Castro R, Rodrigues J, Shi X, Tomás H, PAMAM dendrimer/pDNA functionalized-magnetic iron oxide nanoparticles for gene delivery, J. Biomed. Nanotechnol 11 (2015) 1370–1384, 10.1166/jbn.2015.2101. [PubMed: 26295139]

[185]. Bagó JR, Alfonso-Pecchio A, Okolie O, Dumitru R, Rinkenbaugh A, Baldwin AS, Miller CR, Magness ST, Hingtgen SD, Therapeutically engineered induced neural stem cells are tumour-homing and inhibit progression of glioblastoma, Nat. Commun 7 (2016) 10593, , 10.1038/ncomms10593. [PubMed: 26830441]

[186]. Park TG, Jeong JH, Kim SW, Current status of polymeric gene delivery systems, Adv. Drug Deliv. Rev 58 (2006) 467–486, 10.1016/j.addr.2006.03.007. [PubMed: 16781003]

[187]. Suh J, Paik H, Hwang BK, Ionization of poly(ethylenimine) and poly(allylamine) at various pH's, Bioorg. Chem 22 (1994) 318–327, 10.1006/bioo.1994.1025.

[188]. Behr J, The proton sponge: a trick to enter cells the viruses did not exploit, Chimia 51 (1997) 34–36.

[189]. Nel AE, Mädler L, Velegol D, Xia T, Hoek EM, Somasundaran P, Klaessig F, Castranova V, Thompson M, Understanding biophysicochemical interactions at the nano-bio interface, Nat. Mater 8 (2009) 543–557, 10.1038/nmat2442. [PubMed: 19525947]

[190]. Altanerova U, Babincova M, Babinec P, Benejova K, Jakubechova J, Altanerova V, Zduriencikova M, Repiska V, Altaner C, Human mesenchymal stem cell-derived iron oxide exosomes allow targeted ablation of tumor cells via magnetic hyperthermia, Int. J. Nanomedicine 12 (2017) 7923–7936, 10.2147/IJN.S145096. [PubMed: 29138559]

[191]. Muldoon LL, Sàndor M, Pinkston KE, Neuwelt EA, Imaging, distribution, and toxicity of superparamagnetic iron oxide magnetic resonance nanoparticles in the rat brain and intracerebral tumor, Neurosurgery 57 (2005) 785–796, 10.1227/01.NEU.0000175731.25414.4c. [PubMed: 16239893]

[192]. Strohbehn G, Coman D, Han L, Ragheb RR, Fahmy TM, Huttner AJ, Hyder F, Piepmeier JM, Saltzman WM, Zhou J, Imaging the delivery of brain-penetrating PLGA nanoparticles in the brain using magnetic resonance, J. Neuro-Oncol 121 (2015) 441–449, 10.1007/s11060-014-1658-0.

[193]. Hamilton AM, Foster PJ, In vivo magnetic resonance imaging investigating the development of experimental brain metastases due to triple negative breast cancer, Clin. Exp. Metastasis 34 (2017) 133–140, 10.1007/s10585-016-9835-5. [PubMed: 28108861]

[194]. Richard S, Boucher M, Lalatonne Y, Mériaux S, Motte L, Iron oxide nanoparticle surface decorated with cRGD peptides for magnetic resonance imaging of brain tumors, Biochim. Biophys. Acta Gen. Subj 1861 (2017) 1515–1520, 10.1016/j.bbagen.2016.12.020. [PubMed: 28017683]

[195]. Ai P, Wang H, Liu K, Wang T, Gu W, Ye L, Yan C, The relative length of dual-target conjugated on iron oxide nanoparticles plays a role in brain glioma targeting, RSC Adv. 7 (2017) 19954–19959, 10.1039/C7RA02102J.

[196]. Wu VM, Huynh E, Tang S, Uskoković V, Brain and bone cancer targeting by a ferrofluid composed of superparamagnetic iron-oxide/silica/carbon nanoparticles (earthicles), Acta Biomater. (2019), 10.1016/j.actbio.2019.01.064.

[197]. Shevtsov M, Nikolaev B, Marchenko Y, Yakovleva L, Skvortsov N, Mazur A, Tolstoy P, Ryzhov V, Multhoff G, Targeting experimental orthotopic glioblastoma with chitosan-based superparamagnetic iron oxide nanoparticles (CSDX-SPIONs), Int. J. Nanomedicine 13 (2018) 1471–1482, 10.2147/IJN.S152461. [PubMed: 29559776]

[198]. Kaluzova M, Bouras A, Machaidze R, Hadjipanayis CG, Targeted therapy of glioblastoma stem-like cells and tumor non-stem cells using cetuximab-conjugated iron-oxide nanoparticles, Oncotarget 6 (2015) 8788–8806, 10.18632/oncotarget.3554. [PubMed: 25871395]

[199]. Sallem F, Haji R, Vervandier-Fasseur D, Nury T, Maurizi L, Boudon J, Lizard G, Millot N, Elaboration of trans-resveratrol derivative-loaded superparamagnetic iron oxide nanoparticles for glioma treatment, Nanomaterials 9 (2019) 287, 10.3390/nano9020287.

[200]. Hamilton AM, Aidoudi-Ahmed S, Sharma S, Kotamraju VR, Foster PJ, Sugahara KN, Ruoslahti E, Rutt BK, Nanoparticles coated with the tumor-penetrating peptide iRGD reduce experimental

breast cancer metastasis in the brain, J. Mol. Med 93 (2015) 991–1001, 10.1007/s00109-015-1279-x. [PubMed: 25869026]

[201]. Hemery G, Genevois C, Couillaud F, Lacomme S, Gontier E, Ibarboure E, Lecommandoux S, Garanger E, Sandre O, Monocore vs. multicore magnetic iron oxide nanoparticles: uptake by glioblastoma cells and efficiency for magnetic hyperthermia, Mol. Syst. Des. Eng 2 (2017) 629–639, 10.1039/C7ME00061H.

[202]. Kale SS, Burga RA, Sweeney EE, Zun Z, Sze RW, Tuesca A, Subramony JA, Fernandes R, Composite iron oxide–Prussian blue nanoparticles for magnetically guided T1-weighted magnetic resonance imaging and photothermal therapy of tumors, Int. J. Nanomedicine 12 (2017) 6413–6424, 10.2147/IJN.S144515. [PubMed: 28919744]

[203]. Marie H, Lemaire L, Franconi F, Lajnef S, Frapart YM, Nicolas V, Frébourg G, Trichet M, Ménager C, Lesieur S, Superparamagnetic liposomes for MRI monitoring and external magnetic field-induced selective targeting of malignant brain tumors, Adv. Funct. Mater 25 (2015) 1258–1269, 10.1002/adfm.201402289.

[204]. Fan C-H, Cheng Y-H, Ting C-Y, Ho Y-J, Hsu P-H, Liu H-L, Yeh C-K, Ultrasound/magnetic targeting with SPIO-DOX-microbubble complex for image-guided drug delivery in brain tumors, Theranostics 6 (2016) 1542–1556, 10.7150/thno.15297. [PubMed: 27446489]

[205]. Luo Y, Yang J, Yan Y, Li J, Shen M, Zhang G, Mignani S, Shi X, RGD-functionalized ultrasmall iron oxide nanoparticles for targeted T 1-weighted MR imaging of gliomas, Nanoscale 7 (2015) 14538–14546, 10.1039/C5NR04003E. [PubMed: 26260703]

[206]. Thawani JP, Amirshaghaghi A, Yan L, Stein JM, Liu J, Tsourkas A, Photoacoustic-guided surgery with indocyanine green-coated superparamagnetic iron oxide nanoparticle clusters, Small 13 (2017) 1701300, , 10.002/smll.201701300.

[207]. Lee C, Kim GR, Yoon J, Kim SE, Yoo JS, Piao Y, In vivo delineation of glioblastoma by targeting tumor-associated macrophages with near-infrared fluorescent silica coated iron oxide nanoparticles in orthotopic xenografts for surgical guidance, Sci. Rep 8 (2018) 11122, , 10.1038/s41598018-29424-4. [PubMed: 30042406]

[208]. Hsu F-T, Wei Z-H, Hsuan YC-Y, Lin W, Su Y-C, Liao C-H, Hsieh C-L, MRI tracking of polyethylene glycol-coated superparamagnetic iron oxide-labelled placenta-derived mesenchymal stem cells toward glioblastoma stem-like cells in a mouse model, Artif. Cells, Nanomed. Biotechnol 46 (sup. 3) (2018) S448–S459, 10.1080/21691401.2018.1499661. [PubMed: 30198338]

[209]. Cheng VW, Soto MS, Khrapitchev AA, Perez-Balderas F, Zakaria R, Jenkinson MD, Middleton MR, Sibson NR, VCAM-1–targeted MRI enables detection of brain micrometastases from different primary tumors, Clin. Cancer Res 25 (2019) 533–543, 10.1158/1078-0432.CCR-18-1889. [PubMed: 30389659]

[210]. Jia G, Han Y, An Y, Ding Y, He C, Wang X, Tang Q, NRP-1 targeted and cargo-loaded exosomes facilitate simultaneous imaging and therapy of glioma in vitro and in vivo, Biomaterials 178 (2018) 302–316, 10.1016/j.biomaterials.2018.06.029. [PubMed: 29982104]

[211]. Barajas RF Jr., Hamilton BE, Schwartz D, McConnell HL, Pettersson DR, Horvath A, Szidonya L, Varallyay CG, Firkins J, Jaboin JJ, Combined iron oxide nanoparticle ferumoxytol and gadolinium contrast enhanced MRI define glioblastoma pseudoprogression, Neuro-Oncol. 21 (2018) 517–526, 10.1093/neuonc/noy160.

[212]. Iv M, Samghabadi P, Holdsworth S, Gentles A, Rezaii P, Harsh G, Li G, Thomas R, Moseley M, Daldrup-Link HE, Quantification of macrophages in high-grade gliomas by using ferumoxytol-enhanced MRI: a pilot study, Radiology 290 (2018) 198–206, 10.1148/radiol.2018181204. [PubMed: 30398435]

[213]. Abakumov MA, Nukolova NV, Sokolsky-Papkov M, Shein SA, Sandalova TO, Vishwasrao HM, Grinenko NF, Gubsky IL, Abakumov AM, Kabanov AV, VEGF-targeted magnetic nanoparticles for MRI visualization of brain tumor, Nanomedicine 11 (2015) 825–833, 10.1016/j.nano.2014.12.011. [PubMed: 25652902]

[214]. Tomitaka A, Arami H, Gandhi S, Krishnan KM, Lactoferrin conjugated iron oxide nanoparticles for targeting brain glioma cells in magnetic particle imaging, Nanoscale 7 (2015) 16890–16898, 10.1039/C5NR02831K. [PubMed: 26412614]

[215]. Grauer O, Jaber M, Hess K, Weckesser M, Schwindt W, Maring S, Wölfer J, Stummer W, Combined intracavitary thermotherapy with iron oxide nanoparticles and radiotherapy as local treatment modality in recurrent glioblastoma patients, J. Neuro-Oncol 141 (2019) 83–94, 10.1007/s11060018-03005-x.

[216]. Wu C, Muroski ME, Miska J, Lee-Chang C, Shen Y, Rashidi A, Zhang P, Xiao T, Han Y, Lopez-Rosas A, Repolarization of myeloid derived suppressor cells via magnetic nanoparticles to promote radiotherapy for glioma treatment, Nanomedicine 16 (2019) 126–137, 10.1016/j.nano.2018.11.015. [PubMed: 30553919]

[217]. Cengelli F, Maysinger D, Tschudi-Monnet F, Montet X, Corot C, Petri-Fink A, Hofmann H, Juillerat-Jeanneret L, Interaction of functionalized superparamagnetic iron oxide nanoparticles with brain structures, J. Pharmacol. Exp. Ther 318 (2006) 108–116, 10.1124/jpet.106.101915. [PubMed: 16608917]

[218]. Nosrati H, Salehiabar M, Attari E, Davaran S, Danafar H, Manjili HK, Green and one-pot surface coating of iron oxide magnetic nanoparticles with natural amino acids and biocompatibility investigation, Appl. Organomet. Chem 32 (2018) e4069, , 10.1002/aoc.4069.

[219]. Nikolovski D, Dugalic S, Pantic I, Iron oxide nanoparticles decrease nuclear fractal dimension of buccal epithelial cells in a time-dependent manner, J. Microsc 268 (2017) 45–52, 10.1111/jmi.12585. [PubMed: 28543185]

[220]. Petters C, Irrsack E, Koch M, Dringen R, Uptake and metabolism of iron oxide nanoparticles in brain cells, Neurochem. Res 39 (2014) 1648–1660, 10.1007/s11064-014-1380-5. [PubMed: 25011394]

[221]. Tadic M, Panjan M, Damnjanovic V, Milosevic I, Magnetic properties of hematite (α-Fe2O3) nanoparticles prepared by hydrothermal synthesis method, Appl. Surf. Sci 320 (2014) 183–187, 10.1016/j.apsusc.2014.08.193.

[222]. Lewis CS, Torres L, Miyauchi JT, Rastegar C, Patete JM, Smith JM, Wong SS, Tsirka SE, Absence of cytotoxicity towards microglia of iron oxide (αFe2O3) nanorhombohedra, Toxicol. Res 5 (2016) 836–847, 10.1039/C5TX00421G.

[223]. Wu H-Y, Chung M-C, Wang C-C, Huang C-H, Liang H-J, Jan T-R, Iron oxide nanoparticles suppress the production of IL-1beta via the secretory lysosomal pathway in murine microglial cells, Part. Fibre Toxicol 10 (2013) 46, 10.1186/1743-8977-10-46. [PubMed: 24047432]

[224]. Coccini T, Caloni F, Ramírez Cando LJ, De Simone U, Cytotoxicity and proliferative capacity impairment induced on human brain cell cultures after short-and long-term exposure to magnetite nanoparticles, J. Appl. Toxicol 37 (2017) 361–373, 10.1002/jat.3367. [PubMed: 27480414]

[225]. Phenrat T, Long TC, Lowry GV, Veronesi B, Partial oxidation ("aging") and surface modification decrease the toxicity of nanosized zerovalent iron, Environ. Sci. Technol 43 (2009) 195–200, 10.1021/es801955n. [PubMed: 19209606]

[226]. Orlando A, Colombo M, Prosperi D, Gregori M, Panariti A, Rivolta I, Masserini M, Cazzaniga E, Iron oxide nanoparticles surface coating and cell uptake affect biocompatibility and inflammatory responses of endothelial cells and macrophages, J. Nanopart. Res 17 (2015) 351, , 10.1007/s110510-15-3148-5.

[227]. Chiarelli PA, Revia RA, Stephen ZR, Wang K, Jeon M, Nelson V, Kievit FM, Sham J, Ellenbogen RG, Kiem H-P, Zhang M, Nanoparticle biokinetics in mice and nonhuman primates, ACS Nano 11 (2017) 9514–9524, 10.1021/acsnano.7b05377. [PubMed: 28885825]

[228]. Petters C, Dringen R, Accumulation of iron oxide nanoparticles by cultured primary neurons, Neurochem. Int 81 (2015) 1–9, 10.1016/j.neuint.2014.12.005. [PubMed: 25510641]

[229]. Petters C, Thiel K, Dringen R, Lysosomal iron liberation is responsible for the vulnerability of brain microglial cells to iron oxide nanoparticles: comparison with neurons and astrocytes, Nanotoxicology 10 (2016) 332–342, 10.3109/17435390.2015.1071445. [PubMed: 26287375]

[230]. Hare D, Ayton S, Bush A, Lei P, A delicate balance: iron metabolism and diseases of the brain, Front. Aging Neurosci 5 (34) (2013), 10.3389/fnagi.2013.00034.

[231]. Levy M, Lagarde F, Maraloiu VA, Blanchin MG, Gendron F, Wilhelm C, Gazeau F, Degradability of superparamagnetic nanoparticles in a model of intracellular environment: follow-up of magnetic, structural and chemical properties, Nanotechnology 21 (39) (2010) 395103, , 10.1088/09574484/21/39/395103.

[232]. Voinov MA, Pagán JOS, Morrison E, Smirnova TI, Smirnov AI, Surface-mediated production of hydroxyl radicals as a mechanism of iron oxide nanoparticle biotoxicity, J. Am. Chem. Soc 133 (1) (2010) 35–41, 10.1021/ja104683w. [PubMed: 21141957]

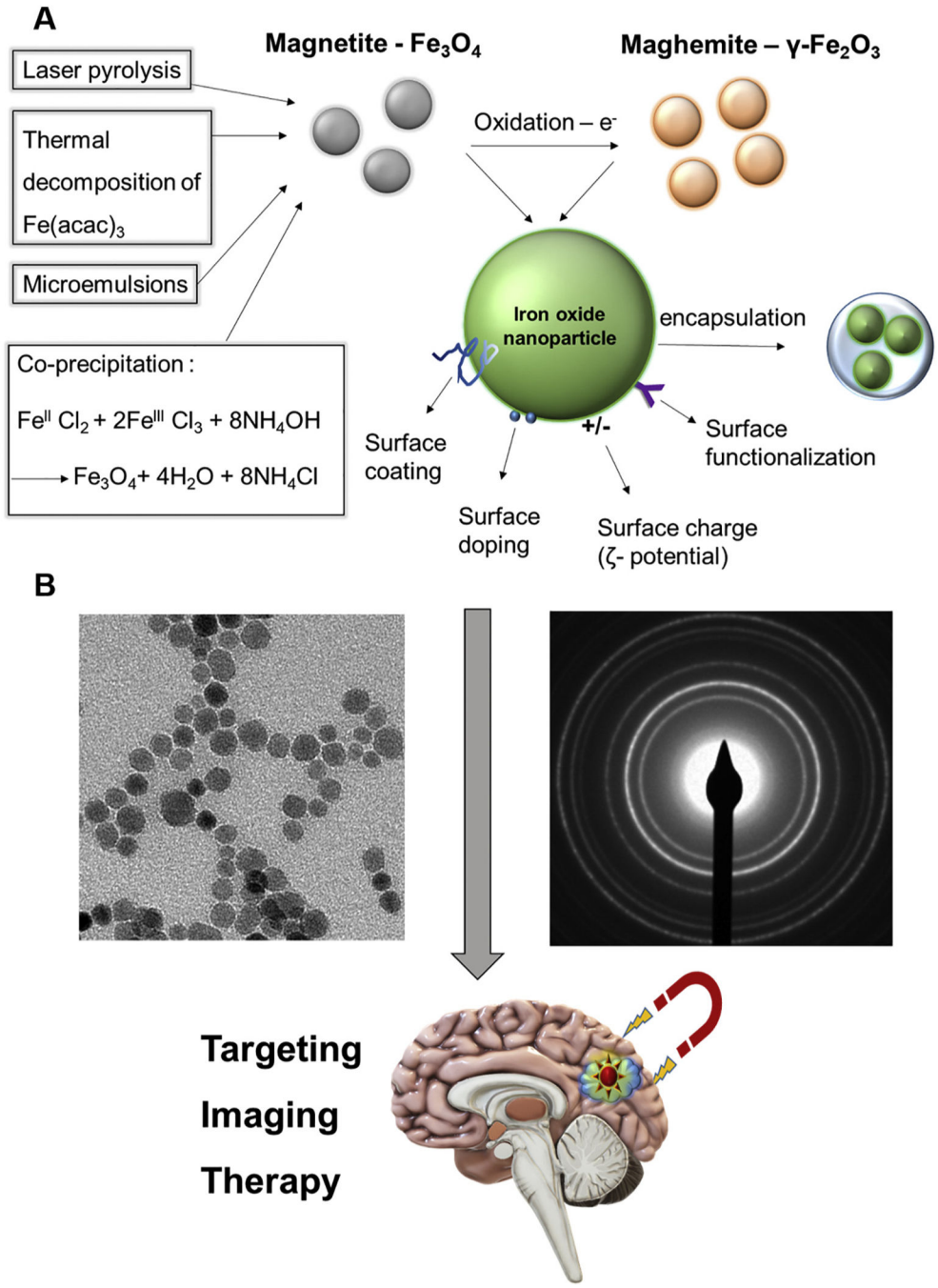

Fig. 1.

Schematic representation of the main fabrication techniques and modifications for biomedical use of iron oxide nanoparticles. A) Magnetite (Fe_3O_4, gray) can be obtained by several methods: co-precipitation, thermal decomposition of iron acetyl acetonate ($Fe(acac)_3$), microemulsions, or laser pyrolysis. Maghemite (γ-Fe_2O_3, orange) can be produced by direct oxidation of magnetite. These nanoparticles (green) can then be modified for biomedical use by methods that include coating, doping or functionalization of the surface as well as encapsulation or altering the surface charge (ζ potential). B: representative

transmission electron microscope (TEM) image (left) and SAED pattern (right) of iron oxide nanoparticles towards potential biomedical applications (bottom).

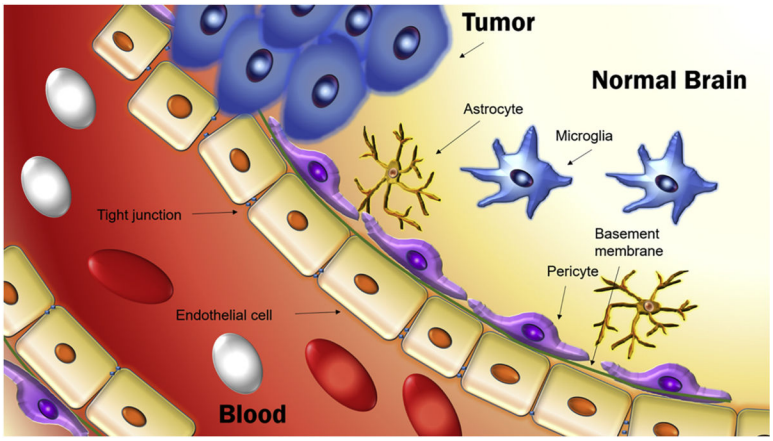

Fig. 2.

Schematic representation of the structure of the blood-brain barrier. Blood vessels in the central nervous system (CNS) are formed primarily by endothelial cells. The endothelial cells are connected to each other by tight junctions and to pericytes by a common basement membrane. The blood-brain barrier is compromised in brain tumors.

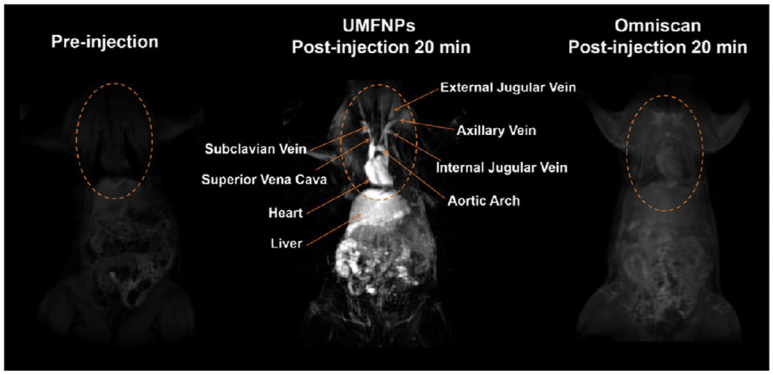

Fig. 3.

Ultrasmall magnetic ferrite nanoparticles (UMFNPs, $MnFe_2O_4$) used as a positive contrast agent enhance magnetic resonance (MR) images. The images show coronal planes obtained *in vivo* in rats using a 3d-flash sequence. Reprinted (adapted) with permission from ref. 69 (ACS Nano, 11 (2017) 3614–3631). Copyright (2017) American Chemical Society.

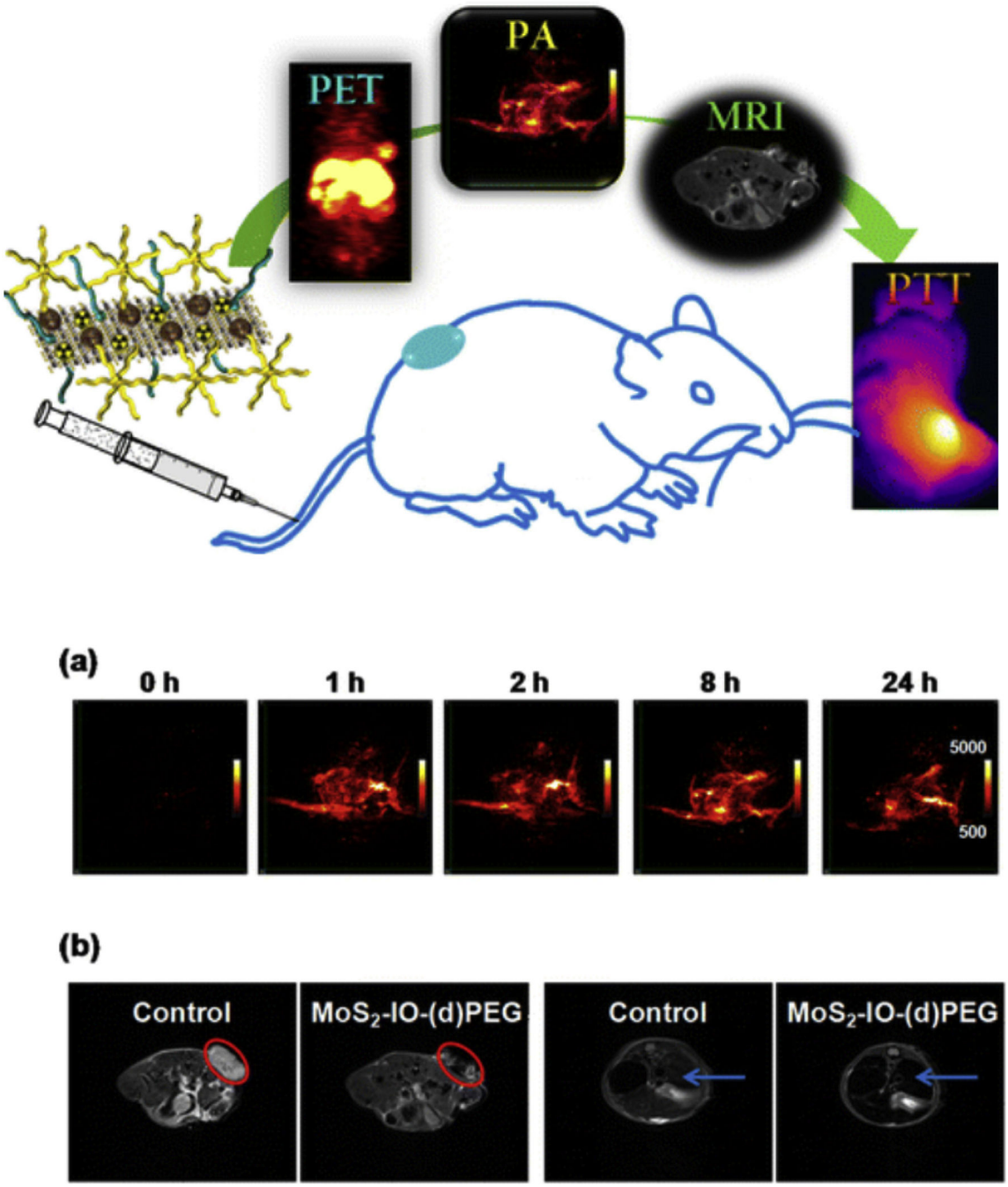

Fig. 4.

A graphical abstract representing the abilities of MoS_2-IO-PEG for positron emission tomography (PET), photoacoustic tomography (PAT), magnetic resonance imaging (MRI) and photothermal therapy (PTT). (a) Photoacoustic tomography (PAT) images of 4T1 tumors in mice acquired before and at various time points after intravenous injection with MoS_2-IO-(d)PEG (dose of MoS_2 = 6.85 mg/kg). (b) T2-weighted MR images showing the transverse sections of a tumor-bearing mouse before and after injection with MoS_2-IO-(d)PEG (dose of MoS_2 = 6.85 mg/kg). The red circles and blue arrows highlight the 4T1 tumor and liver of

mice, respectively. MoS_2-IO-PEG, molybdenum disulfide iron oxide polyethylene glycol. Reprinted (adapted) with permission from ref. 164 (ACS Nano, 9 (2015) 950–960). Copyright (2015) American Chemical Society.

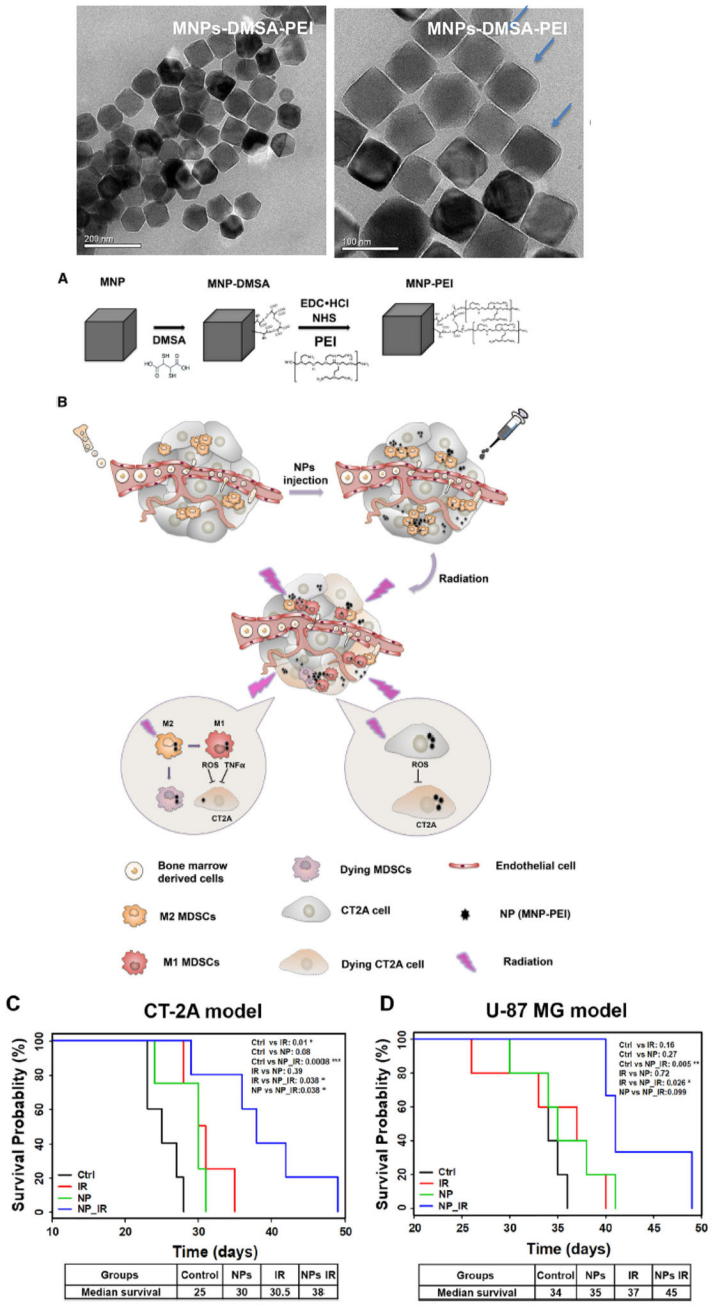

Fig. 5.

Schematic representation of the synthesis of nanoparticles (NPs) and their effects on tumor cells and animal survival. (A) Transmission electron microscopy (TEM) images of MNPs-DMSA-PEI (above) and steps in the synthetic process (below). (B) NPs lead specifically to severe tumor cell toxicity. MDSCs are partially jeopardized as well as repolarized into M1-like phenotype generating an antitumor effect after NPs with radiation treatment. The synergistic effect resulted in effective anti-tumor efficacy. (C) Cumulative survival curve (Kaplan–Meier survival plot) of C57/BL6 mice (n = 5 mice in each group). CT-2A cells

were intracranially (i.c.) implanted and allowed to establish for a week. Mice in IR and NP_IR groups were then treated with radiation from day 8 to 11 (2 Gy per day). (D) Cumulative survival curve (Kaplan–Meier survival plot) of nude mice implanted with U-87 MG cells. Mice in IR and NP_IR groups received 4 Gy radiation (2 Gy each day) post 24 h of PBS or NPs injection. The overall P value was calculated by the log-rank test. Significance levels of P values are marked in the plots (*P < 0.05; **P < 0.01; ***P < 0.001). DMSA, di-mercaptosuccinic acid; EDC, 1-Ethyl-3-(3-dimethylaminopropyl) carbodiimide; IR, radiation treatment; MDSCs, myeloid derived suppressor cells; MNP, magnetic nanoparticle; NHS,N-hydroxysuccinimide; PEI, polyethylene imine; ROS, reactive oxygen species; TNFα, tumor necrosis factor alpha. Reprinted from ref. 216: Repolarization of myeloid derived suppressor cells via magnetic nanoparticles to promote radiotherapy for glioma treatment, Wu et al., Nanomed. Nanotechnol. Biol. Med., 16 (2019) 126–137, Copyright (2019), with permission from Elsevier.

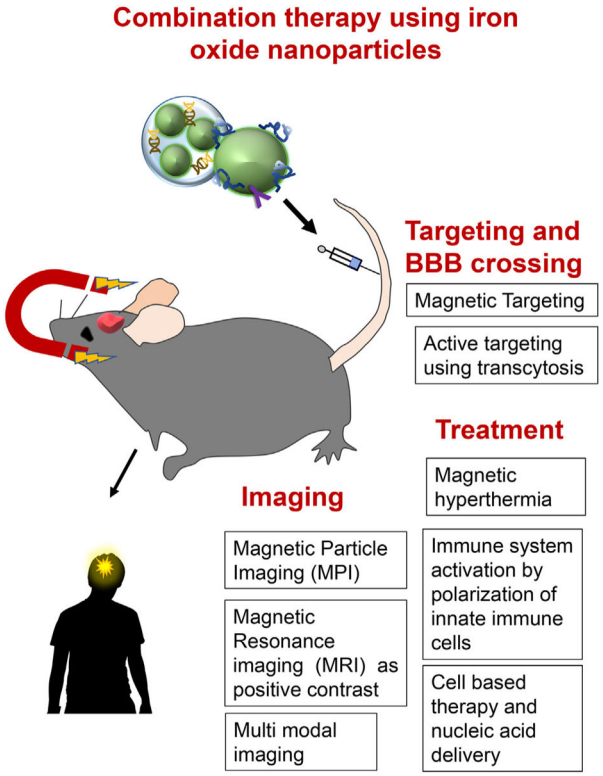

Fig. 6.

Summary of future directions for clinical use of iron oxide nanoparticles (IONPs). Promising future biomedical applications of IONPs include imaging (MPI, positive contrast agent in MRI, multimodal imaging), magnetic/active targeting and blood-brain barrier (BBB) crossing and treatment (magnetic hyperthermia, activation of immune system by immune cell polarization, cell based therapy and nucleic acid delivery).

Table 1

Summary of studies using iron oxide nanoparticles for brain tumor applications.

Application	Type of study	References
Imaging		
MRI (Negative contrast)	preclinical model	[64,192–195,203–204,206–209,209–210,213,102–103,105,126,174]
MRI (Positive contrast)	preclinical model	[202,205]
MRI	clinical, human patients	[211,212]
MPI	preclinical model	[214]
Targeting		
Magnetic targeting	preclinical model	[8,196–199,203–204,93,102,89]
Treatment		
Delivery of therapeutic molecules	preclinical model	[199–200,206,209–210]
Magnetic hyperthermia	preclinical model	[201]
Magnetic hyperthermia	clinical, human patients	[215]
Cell based	preclinical model	[209,208,216]